EARTHQUAKE ENGINEERING RESEARCH CENTRE
UNIVERSITY OF ICELAND
AUSTURVEGUR 2A, 800 SELFOSS

EARTHQUAKE HAZARD

Preliminary assessment for an industrial lot at Bakki near Húsavík

Ragnar Sigbjörnsson
Jónas Thór Snæbjörnsson

Report No. 07001, Selfoss 2007

Ragnar Sigbjörnsson and Jónas Thór Snæbjörnsson: *Earthquake hazard - Preliminary assessment for an industrial lot at Bakki near Húsavík.* Earthquake Engineering Research Centre, University of Iceland, Report No. 07001, Selfoss 2007.

ABSTRACT

This report presents a preliminary probabilistic seismic hazard analysis addressing an industrial lot at Bakki, near Húsavík, in North Iceland. The analysis is applied to obtain peak ground acceleration values and spectral acceleration response ordinates corresponding to 10% probability of exceedance in 50 years, as well as other probabilistic reference values that may be of use in design. The inelastic structural behaviour has also been studied and spectral acceleration response ordinates for stiff and flexible system, respectively, are presented.

It should be noted that the duration of strong shaking is relatively short for the study site. The dynamic amplification of earthquake induced response tends to be higher for distant events with the long duration, than for closer events with shorter durations. The rapid attenuation of spectral acceleration ordinates with increasing source distance is also pointed out. These aspects have an effect on both the spectral acceleration ordinates and the structural behaviour factors. It is worth underlining that the result is a significant reduction in computational earthquake design action compared to using the uncalibrated box table values provided in Eurocode 8.

Finally further earthquake hazard studies are suggested and outlined.

TABLE OF CONTENTS

1. INTRODUCTION

The study presented herein is a preliminary assessment of the seismic hazards and earthquake action on the proposed industrial lot at Bakki near Húsavík in North Iceland (66.08°N, 17.34°W). The objective of the study is to define preliminary earthquake design provisions to be applied in a feasibility study. The main emphasis is placed on the following topics:

- Hazard curves for peak ground acceleration for selected return periods.
- Hazard curves for elastic response spectrum ordinates of horizontal and vertical acceleration for selected range of undamped natural periods and 5% critical damping ratio.
- Preliminary hazard curves for inelastic response spectrum ordinates for two selected natural periods, constant ductility ratio and 5% critical damping ratio.
- Preliminary design specifications for selected return periods in the form of an elastic design spectrum and summary of appropriate consideration of inelastic effects.

The objective of an earthquake hazard analysis is to quantify the level of ground motion at the site due to earthquakes. The ground motion can be the intensity of the earthquake, displacement, velocity or acceleration of the seismic wave at the site. Seismic hazard is determined by the following three factors:

- The distribution in time, space and size of the regional seismicity
- The attenuation of seismic waves from the location of the earthquake
- The action of the shallow geology in the distortion of the seismic signal

The hazard can be estimated using deterministic or probabilistic methods (Cornell 1968). Probabilistic methods entail evaluating the probability of exceeding a particular level of ground motion (such as a certain value of peak acceleration) at a site during a specific time interval (such as 50 years). The three major elements of the probabilistic method are:

- the characterisation of seismic sources by:
  - compilation of an earthquake catalogue
  - delineation of the seismic sources
  - magnitude-frequency distribution
- the characterisation of attenuation of ground motion, described by attenuation functions
- computation of the probability analysis

The analysis must incorporate the inherent uncertainty of the size, location, and time of occurrence of future earthquakes, and the attenuation of seismic waves as they propagate from all possible sources in the region to all possible sites. For this purpose probability functions are required for:

- the magnitude,
- the distance to earthquake source,
- the strong ground motion estimation relations.

The following chapters will discuss the above mentioned elements of a probabilistic hazard analysis. A short review of the seismic sources involved and the available earthquake catalogue is given in chapter 2 along with a discussion of Icelandic attenuation characteristics. Models for estimating earthquake motion are briefly discussed in chapter 3 and the regression models applied in this study introduced. The fundamentals of the probabilistic seismic hazard analysis are presented in chapter 4. The corresponding design specifications suggested are given in chapter 5, along with few comments emphasising the importance of a conceptual design approach.

2. SEISMICITY

2.1 General description

Iceland is a super-structural part of the Mid Atlantic Ridge marking the boundary between the North American and the Euro-Asian Plate. The Ridge can be visualised as a belt of seismic activity. At the Reykjanes Peninsula the plate boundary is seen as a seismic delineation centring the Reykjanes Seismic Zone (RSZ). Across Iceland from southwest to the north, the plate boundary is displaced to the east through two major fracture zones, the South Iceland Seismic Zone (SISZ) in the lowlands of the south and the Tjörnes Fracture Zone in the north (North Iceland Seismic Zone, NISZ), which is mostly located offshore. The largest historic earthquakes in Iceland have occurred within these zones the size of which have exceeded magnitude 7. The focal mechanism of these earthquakes is characteristically a strike-slip faulting, which is consistent with transform fault interpretation. The clear topographic expression characteristic of fracture zones on the ocean floor is missing, however, and in neither zone is the transform motion taken up by a single major fault. Beside these three main regions of seismic activity, intraplate earthquakes have occurred in the western and north-western part of the country and also off the East Coast. These earthquakes are not expected to exceed magnitude 5½-6. Furthermore, seismic activity of lesser magnitude but greater frequency is observed in the in the volcanic zones. The main features of the seismo-tectonics are summarised in Figure 2.1 below. A more detailed overview can be found in Einarsson (1991) and Bourgeois et al. (1998).

2.2 Earthquake source zones

The North Iceland Seismic Zone is a broad region of faulting and seismic activity, which connects the submarine Kolbeinsey Ridge and the volcanic zone in North Iceland at Öxarfjörður[1]. Earthquake epicenters are scattered throughout the region, which is about 80 km wide from north to south and 150 km long between Melrakkaslétta in the east to Skagi in the west. There is a concentration of epicenters in the northeastern part of the zone indicating higher activity than in the western part. The seismic character of the zone is complex and cannot be associated with a single fault or plate boundary. Studies of recent earthquakes show that a considerable part of the seismicity is associated with three hypothetical parallel WNW trending lines, visualised as seismic delineations.

[1] Sæmundsson, K., Karson, A,K. (2006): Stratigraphy and Tectonics of the Húsavík-Western Tjörnes Area. ÍSOR-2006/032, 2006.

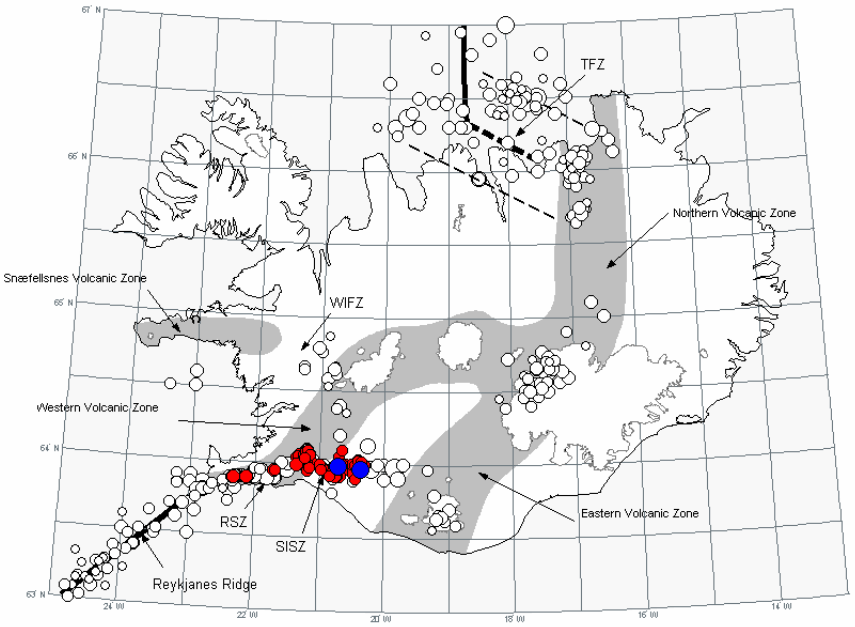

Figure 2.1 – Main tectonic structures and earthquake epicentres: The grey areas indicate volcanic zones; solid lines indicate rift zones offshore representing parts of the Mid-Atlantic Ridge; the rift zones on land are located at the Eastern, the Western and the Northern Volcanic zones; dashed lines indicates fracture zones offshore and seismic lineation; SISZ is the South Iceland Seismic Zone; TFZ is the Tjörnes Fracture Zone; WIFZ is the West Iceland fracture Zone; white circles denote earthquake epicentres (Ambraseys and Sigbjörnsson, 2000); red circles show epicentres of events recorded by the Icelandic Strong-motion Network during the South Iceland earthquake sequence in June 2000 and the blue circles denote the two largest events in June 2000 (http://www.ISESD.hi.is).

The first of these, counting from north-east, is the Grimsey seismic delineation that runs slightly north of Grímsey and joins the Krafla fissure swarm in Axarfjördur. It has not a clear trace in the topography. Instead, the surface structure is characterized by northerly trending troughs and ridges. In some respect this resembles the structure in the SISZ where the epicentral belt lacks clear surface manifestation.

The second seismic delineation, which runs NWN from Húsavík across Flatey and north of Eyjafjördur. The 1872 magnitude 6½ earthquake originated within this delineation. It caused widespread damage in Húsavík, Flatey and Flateyjardalur.

The third assumed seismic delineation runs NWN from Krafla Central Volcano across Eyjafjördur near Dalvík and to the mouth of Skagafjördur. Magnitude 7 earthquake occurred in the mouth of Skagafjördur on this third delineation in 1963. As is the case with most historic earthquakes in the NISZ, the epicentre was off the coast in the ocean and the land intensity therefore low to moderate. The earthquake caused alarm and some damage in the nearby town of Saudárkrókur.

2.3 Characterisation of seismic sources - Earthquake catalogue

The characterisation of seismic sources, involves quantifying three physical parameters of a potential seismic source:

1. geometry and location of the source (or fault), (where do earthquakes occur?)
2. rate of earthquake recurrence (how often do earthquakes occur?) and
3. maximum magnitude, (how big can we expect theses earthquakes to be?).

Seismicity catalogues are the fundamental data base used to determine where, how often, and how big earthquakes are likely to be. However seismicity statistics are generally based on geologically short catalogues. Therefore the information from seismic monitoring, historic records, geodetic monitoring, and geologic records are combined to characterise seismic sources. These data, when available, are used to interpret seismic source zones. Because different interpretations of the input data are possible, large uncertainties are often associated with source characterisation.

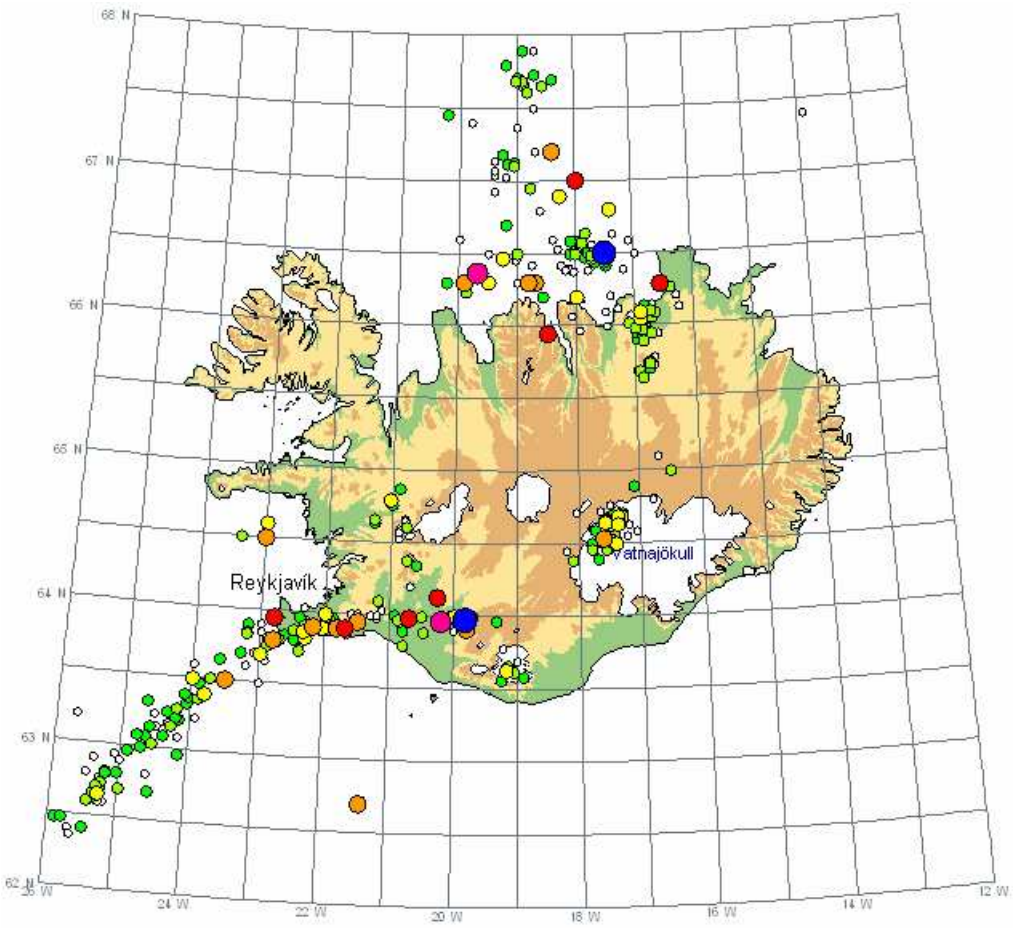

Figure 2.2 - Spatial distribution of earthquake epicentres in the Parametric Earthquake Catalogue for Iceland for the period 1896 to 1996 (Ambraseys and Sigbjörnsson, 2000). The following colour code is used: blue - $M_W \in [7.0; 7.5]$; purple - $M_W \in [6.5; 7.0]$; red - $M_W \in [6.0; 6.5]$; orange - $M_W \in [5.5; 6.0]$; yellow - $M_W \in [5.0; 5.5)$; yellow-green - $M_W \in [4.5; 5.5]$; green - $M_W \in [4.0; 4.5]$; white - $M_W \in [3.0; 4.0]$ or undefined.

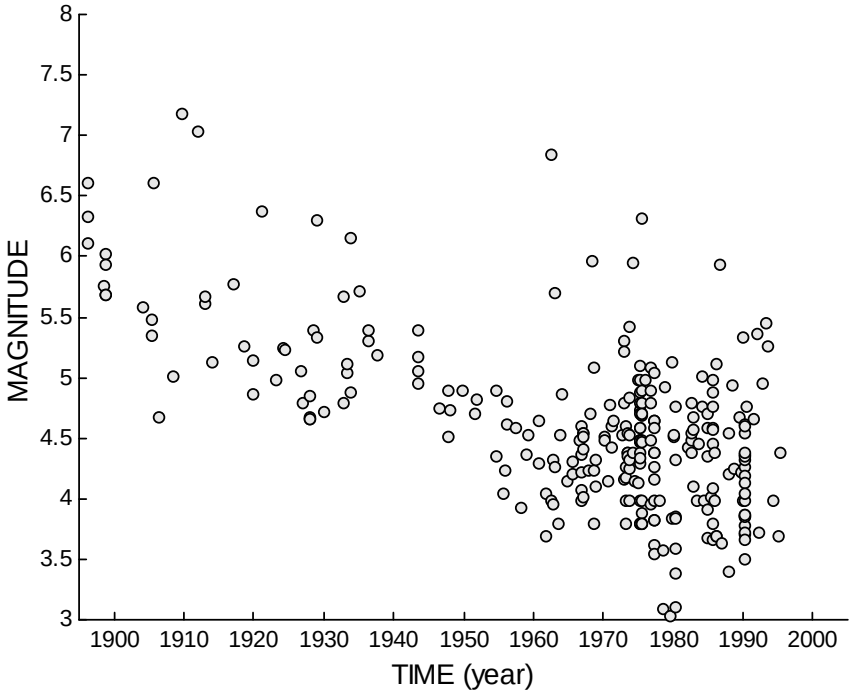

Figure 2.3 - Time-line of the Parametric Earthquake Catalogue for Iceland showing surface-wave magnitude as a function of time.

A Parametric Earthquake Catalogue for Iceland has been compiled by Ambraseys and Sigbjörnsson (2000). The study area is defined as the area between the latitudes 62°N and 68°N and the longitudes 12°W and 26°W. The time period spanned by the catalogue is one century, i.e. from 1896 to 1996. The selection of the starting year for the catalogue is the fact, that the first earthquake in Iceland for which there is available instrumental data is the destructive 1896 South Iceland Earthquake. The magnitude scale applied is the surface-wave magnitude scale. Total number of events in the compiled catalogue is 422, including 276 events with recalculated surface-wave magnitude.

The geographical distribution of earthquakes is shown in Figure 2.2, including all events. The circles denote earthquake epicentres, as previously, applying an extended colour code as well as the size of the circles to visualise the earthquake magnitude. The time-line of earthquake activity, as furnished in the events with recalculated surface-wave magnitude, is depicted in Figure 2.3.

The catalogue can be regarded as complete during the whole period for events with magnitudes exceeding roughly 4½ which is normally considered satisfactory for engineering hazard assessment. Furthermore, the catalogue seems to cover the main earthquake areas fairly.

2.4 Rate of earthquake recurrence and Maximum magnitudes

The activity of each source is described by frequency-magnitude occurrence relationship. The rate of recurrence of earthquakes on a seismic source is assumed to follow the Gutenberg-Richter relation, expressed herein as:

$$n = a\exp(-bM) \tag{2.1}$$

where n is the number of events per year having magnitudes greater than M and a and b are constants defined by regression analysis. The slope of the magnitude-frequency Gutenberg-Richter defines the "b-value" parameter**.** For a single source, the modified (double truncated) Gutenberg-Richter relation is

$$N = a_n\left[\left(1-\exp\left(-b\left(M-M_{\min}\right)\right)\right)/\left(1-\exp\left(-b\left(M_{\max}-M_{\min}\right)\right)\right)\right] \tag{2.2}$$

$M_{\max}$ and $M_{\min}$ are the upper and lower bound magnitude on the source, a_n is the total number of events in a closed magnitude intermal [$M_{\min}$: $M_{\max}$]. $M_{\min}$, is the magnitude below which no engineering-significant damage is expected and $M_{\max}$ represents the maximum expected magnitude. The maximum magnitude is related to the tectonic setting, geometry, and type of the seismic source. To characterise each source zone, the following parameters are evaluated:

- $M_{\max}$ and $M_{\min}$, the upper and lower bound magnitude on the source
- the Gutenberg-Richter earthquake recurrence parameter (β-value)
- the activity rate α_n the number of event per year having magnitudes equal to or greater than $M_{\min}$ on the source, and additionally
- the average hypocentral depth

It is clear that the presented parametric earthquake catalogue contains different types of earthquakes occurring within our study area. For instance, it seems obvious that the catalogue contains earthquakes related to volcanic activity as well as earthquakes of more direct tectonic origin from at least three fault zones. Based on this observation it is suggested that the magnitude distribution function can be obtained by approximating the parent earthquake population as a mixture of, at least, two different, exponentially distributed populations. The compound density function of the total data set can be expressed as:

$$n = \begin{cases} a_1\exp(-b_1M) + a_2\exp(-b_2M); & M_{1,\min} \le M < M_{2,\max} \\ \chi_2; & M_{2,\max} \le M < M_{2,\max} + \Delta M \end{cases} \tag{2.3}$$

Here, $M_{1,min}$, $M_{1,max}$, $M_{2,min}$, $M_{2,max}$, ΔM, α_1, β_1, α_2, β_2 and χ_2 are model parameters. The parameter χ_2 is included to account for uncertainties in the magnitude determination.

The cumulative distribution derived from Eq. (3) is given as follows:

$$N = \begin{cases} \dfrac{a_1}{b_1}\left(\exp(-b_1 M) - \exp(-b_1 M_{1,\max})\right) \\ \quad + \dfrac{a_2}{b_2}\left(\exp(-b_2 M) - \exp(-b_2 M_{2,\max})\right) + \chi_2 \, \Delta M; \quad M_{1,\min} \le M < M_{2,\max} \\ \chi_2 \, (M_{2,\max} + \Delta M - M); \qquad\qquad M_{2,\max} \le M < M_{2,\max} + \Delta M \end{cases} \tag{2.4}$$

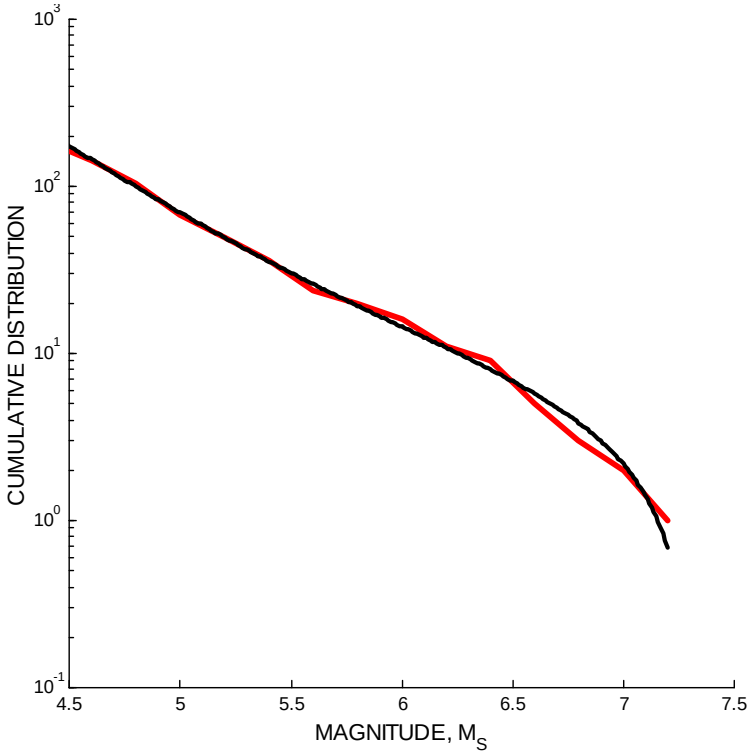

Figure 4 – A cumulative distribution of earthquakes within the study area. The red curve is an empirical distribution derived from the parametric earthquake catalogue and the black curve is obtained by regression analysis. The parameters obtained are: α_1 = 15.1431, β_1 = 2.079, α_2 = 2.1301, β_2 = 0.047305, $\max(M_S) = M_{max}$ = 7.2976.

Figure 2.4 displays the fitted distribution, Eq.(2.4), along with the empirical magnitude distribution as derived from the parametric catalogue. The corresponding density function, Eq.(2.3) is plotted in Figure 2.5 along with the empirical data. The fit seems to be reasonable, even though the log-scale distorts the "vision". It should also be clear after visual inspection of Figure 2.4 and 2.5 that the suggested compound distribution fits the data betted than a traditional exponential distribution.

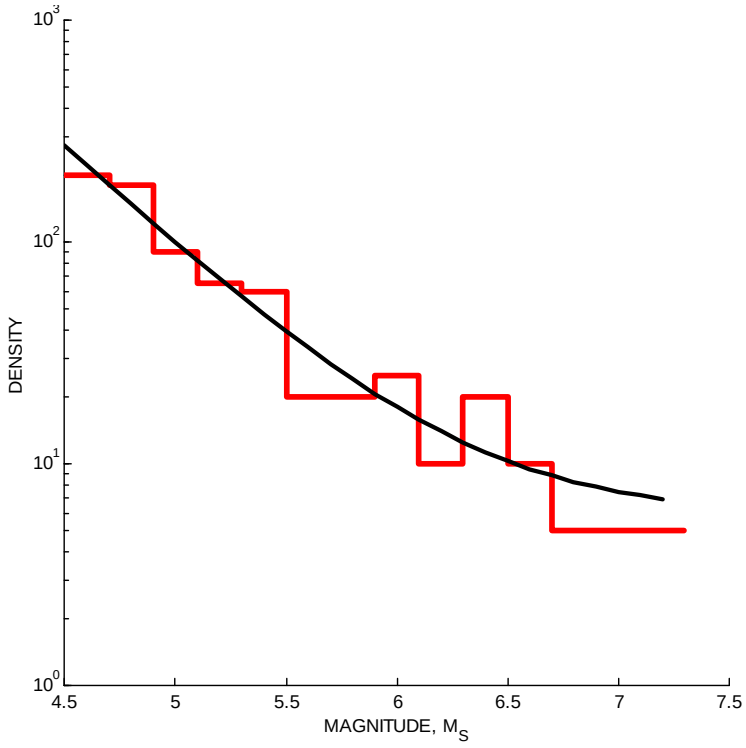

Figure 5 – A density distribution of earthquakes within the study area. The red curve is an empirical distribution derived from the parametric earthquake catalogue and the black curve is obtained by regression analysis. The parameters obtained are: a_1 = 15.1431, b_1 = 2.079, a_2 = 2.1301, b_2 = 0.047305, max(M_S) = M_{max} = 7.2976.

2.5 Characterisation of attenuation of ground motion

Estimates of expected ground motion at a given distance from an earthquake of a given magnitude are the second element of earthquake hazard assessments. These estimates are usually equations, called attenuation relationships, which express the expected ground motion as a function of distance for a given magnitude (and occasionally other variables, such as type of faulting). Ground motion attenuation relationships may be determined in two different ways: empirically, using previously recorded ground motions, or theoretically, using seismological models to generate synthetic ground motions which account for the source, site, and path effects. However, there is an overlap in these approaches, since empirical approaches fit the data to a functional form suggested by theory and theoretical approaches often use empirical data to determine some parameters.

The ground motion at a site depends on the earthquake source, the seismic wave propagation and the site response. Earthquake source signifies the earthquake magnitude, the depth and the focal mechanism, the propagation depends mainly on the distance to the site. The site response deals with the local geology (site classification: hard rock, soft rock, etc.). Hazard values calculated for rock/stiff soil sites (the most common site classifications) are lower than hazard values calculated for soil sites.

Attenuation in Iceland is faster than predicted by most of the common attenuation models found in the literature (see for instance Douglas, 2003 and 2004). This is a

well established property of Icelandic earthquakes and is believed to be related to the geological properties of the Icelandic crust and the characteristics of Icelandic earthquakes. The crust is relatively young in geological terms, heterogeneous and cracked. This results in higher anelastic attenuation than found in the continental crusts. The largest earthquakes in Iceland originating in the above mentioned fracture zones are characterised as shallow strike-slip earthquakes with a vertical fault plane rupturing to the surface for moderate sized events. These results in a narrow near source zone where the peak ground acceleration is roughly constant for a given event (see Figure 1). For a magnitude 6½ event the size of this near source zone is limited to an area stretching 5 to 6 km from the surface trace of the causative fault. In the intermediate field the attenuation is faster than in the far field where it is found to be inverse proportional to the source distance. For the above mentioned moderate sized event the horizontal peak ground acceleration has attenuated down to approximately 15% g at a 15 km distance from the surface trace of the causative fault (see Sigbjörnsson and Ólafsson, 2004).

3. STRONG-MOTION ESTIMATION MODELS

3.1 General remarks

The term strong-motion estimation models refer on one hand to the so-called ground motion estimation model and on the other hand to the earthquake response spectrum estimation model. They can be used to obtain characteristic quantities like peak ground acceleration and response spectrum acceleration. Furthermore, they are also used to generate synthetic accelerograms and time series for ground motion and structural response.

The methods and models outlined in this chapter are the basis for the probabilistic seismic analysis presented in the following Chapter.

The ground motion estimation models, often referred to as attenuation models or attenuation laws, are used to obtain values for quantities used to describe the ground motion at a given site induced by earthquakes in a surrounding seismogenic region. These models can be divided into two main classes. Firstly, there are theoretical models, which are derived using the basic principles of mechanics. Secondly, we have models derived using regression analysis, which in principle consists of fitting an optimal model to a predefined strong-motion data set.

Strong-motion estimation models derived by regression analysis are more common in engineering applications than the theoretical models. A comprehensive overview of the available range of regression type models has been given by Douglas (2004). The reliability of these models relies heavily on the data set applied to derive the model parameters although the functional form is also an important factor.

Earthquake response spectrum estimation models are of fundamental importance in aseismic design of structure and are one of the key tools applied in design codes. Although the response spectrum is defined for single degree-of-freedom systems, it is used in practise for multi-degree-of-freedom systems applying an appropriate superposition principle. Strictly speaking the response spectrum superposition methods are only applicable to linear elastic structures. However, it has been extended to non-linear structures by modifying the input response spectra for different non-linear effects, for instance by introducing the ductility factor as an additional parameter to describe the system behaviour (Newmark and Hall, 1969). Such methods are commonly applied in codified design procedures where the dynamic action, especially for regular structures, is transformed into “statically equivalent loads”.

3.2 Regression type strong-motion estimation models models

In a resent study Ambraseys et al. (2005) derived a new set of regression models for both horizontal and vertical strong motion, which fulfil as far as possible the required model criteria and in addition account for the different faulting mechanism. The applied

data is from the ISESD data bank (http://www.ISESD.hi.is, 2005), which is one of the best available sources for strong ground motion data. Table 3.1 lists the countries of origin, which are from Europe and the Middle East. We see that almost 12% of the records originate from Iceland. Hence, the seismic environment in Iceland should be fairly well represented.

In the models introduced by Ambraseys et al. (2005) the peak ground acceleration, *PGA*, and response spectrum, S_a, are expressed respectively, as follows:

$$PGA = f_G\left(M_w, d, site\,condition, style\ of\ faulting\right)$$
$$S_a = f_R\left(T_n, M_w, d, site\,condition, style\ of\ faulting\right)$$

Here, d is distance from site to source, M_w is moment magnitude and T_n is the undamped natural frequency of the structure.

The functional form adopted in the study of Ambraseys et al. (2005) is given as:

$$\log_{10}\left(S\right) = a_1 + a_2 M_w + (a_3 + a_4 M_w)\log_{10}\sqrt{d^2 + a_5^2} + a_6 S_S + a_7 S_A + a_8 F_N + a_9 F_T + a_{10} F_O \tag{4.1}$$

Here the following notation is used:

a_1 … a_{10} are regression coefficients derived using the data set outlined above,
M_w is moment magnitude (≥ 5),
d is source to site distance in km,
S_S = 1 for soft soil sites and 0 otherwise,
S_A = 1 for stiff soil sites and 0 otherwise,
F_N = 1 for normal faulting earthquakes and 0 otherwise,
F_T = 1 for thrust earthquakes and 0 otherwise and
F_O = 1 for odd faulting earthquakes and 0 otherwise.

This general form is used both for the peak ground acceleration and the response spectral ordinate for both horizontal and vertical motion. Two different sets of regression coefficients are used to represent each component of acceleration. For the spectral ordinates, one set of parameters is derived for each set of undamped natural periods and critical damping ratios.

It should be noted that no data from western North America is used by Ambraseys et al in the derivation of the regression model equations. That decision was, in part, based on the finding of Douglas (2004) that ground motions in Europe and California US data seem to be significantly different. However, when the model was compared with data from the Parkfield earthquake (28th September 2004) it was found to fit the data reasonably well, thus indicating that the differences in ground motions between western North America are perhaps not as significant as would be thought given the analysis of Douglas (2004).

Table 3.1 - Distribution of strong-motion after countries of origin (Ambraseys et al., 2005).

Country	*Number of records*
Italy	174
Turkey	128
Greece	112
Iceland	69
Serbia & Montenegro	24
Iran	17
Slovenia	15
Georgia	14
Armenia	7
Spain	6
Portugal	4
Other countries	25
Total	595

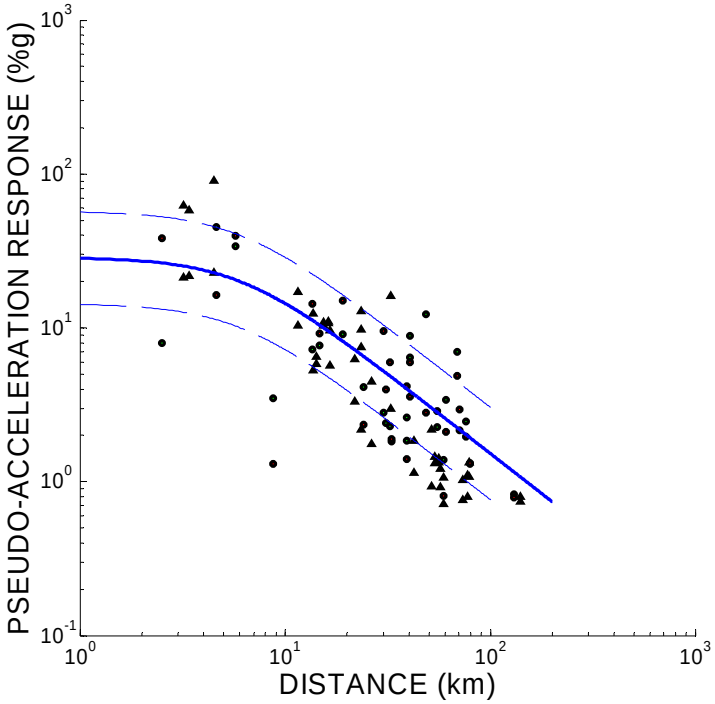

Figure 3.1 – Attenuation of linear elastic spectral acceleration response. Comparison of strong-motion estimation models to data. Undamped natural period is 1.0 s and the critical damping ratio is 5%. The blue curve represents the Ambraseys et al. model (2005), and the blue dashed curves represents ± one standard deviation. The circles and triangles represent data from the South Iceland earthquakes on 17 and 21 June 2000.

Comparison to Icelandic data

Earlier studies, where available regression models have been applied to Icelandic data have indicated slower attenuation than is characteristic for the Icelandic data (Ólafsson, 1999). This is also seen to be the case in Figure 3.1, where the Ambraseys et al. (2005) model is compared to data from the June 2000 earthquakes, as well as a theoretical model discussed in Sigbjörnsson and Ólafsson (2004).

Similar results are obtained for the response spectrum. However, we get generally a better fit for the more flexible structures than for the stiffer ones. A more thorough discussion of the bias can be found in Ambraseys et al. (2005).

4. PROBABILISTIC SEISMIC HAZARD ANALYSIS

4.1 Introduction

The term *seismic hazard* is commonly used to describe potentially damaging phenomena associated with earthquake threats. Most often it is used to describe the phenomena qualitatively by setting up possible scenarios and spelling out potential effects. On the other hand, when the intention is to express quantitatively the likelihood, frequency or probability of occurrence of specified effects at a particular site in a given region the term is commonly referred to as *probabilistic seismic hazard* and the quantitative methodology used named probabilistic seismic analysis.

Probabilistic seismic hazard analysis grew out of the societal needs for improved engineering design. The theoretical foundation of the analysis is based on the framework of structural reliability and safety. The basic elements of the commonly applied mainstream methodology are outlined in Figure 4.1 emphasising the derivation of engineering design criteria for earthquake-induced ground motion. The same methodology applies obviously also to the development of structural design criteria expressed in terms of *uniform hazard spectra* to be used in performance based codified design.

The probabilistic seismic hazard analysis used in contemporary studies is commonly based on the work of Cornell (1968) and McGuire (1978). Furthermore, a good overview can be found in Chen and Scawthorn (2003), especially in Chapter 8 by Tenhaus and Campbell on Seismic Hazard Analysis. The book by McGuire (2004) on Seismic Hazard and Risk Analysis is also worth mentioning, where the state of the art of the methodology is outlined and summarised emphasising the practical aspects from the engineering point of view.

The basic elements of the solution technique fall within the framework of Monte Carlo simulation techniques. The strength of this technique is its simplicity and flexibility in dealing with multiple faults and source zones. In fact no limitation is set on the complexity of modelling the regional or local seismicity. Furthermore, the technique applies both to linear elastic and non-linear inelastic system behaviour and is consistent with methods most commonly used in structural reliability analysis and prediction (Melchers, 2002).

The purpose of this chapter is to outline the applied methodology and present the obtained computational results put forward as hazard curves and uniform hazard spectrum for the study site.

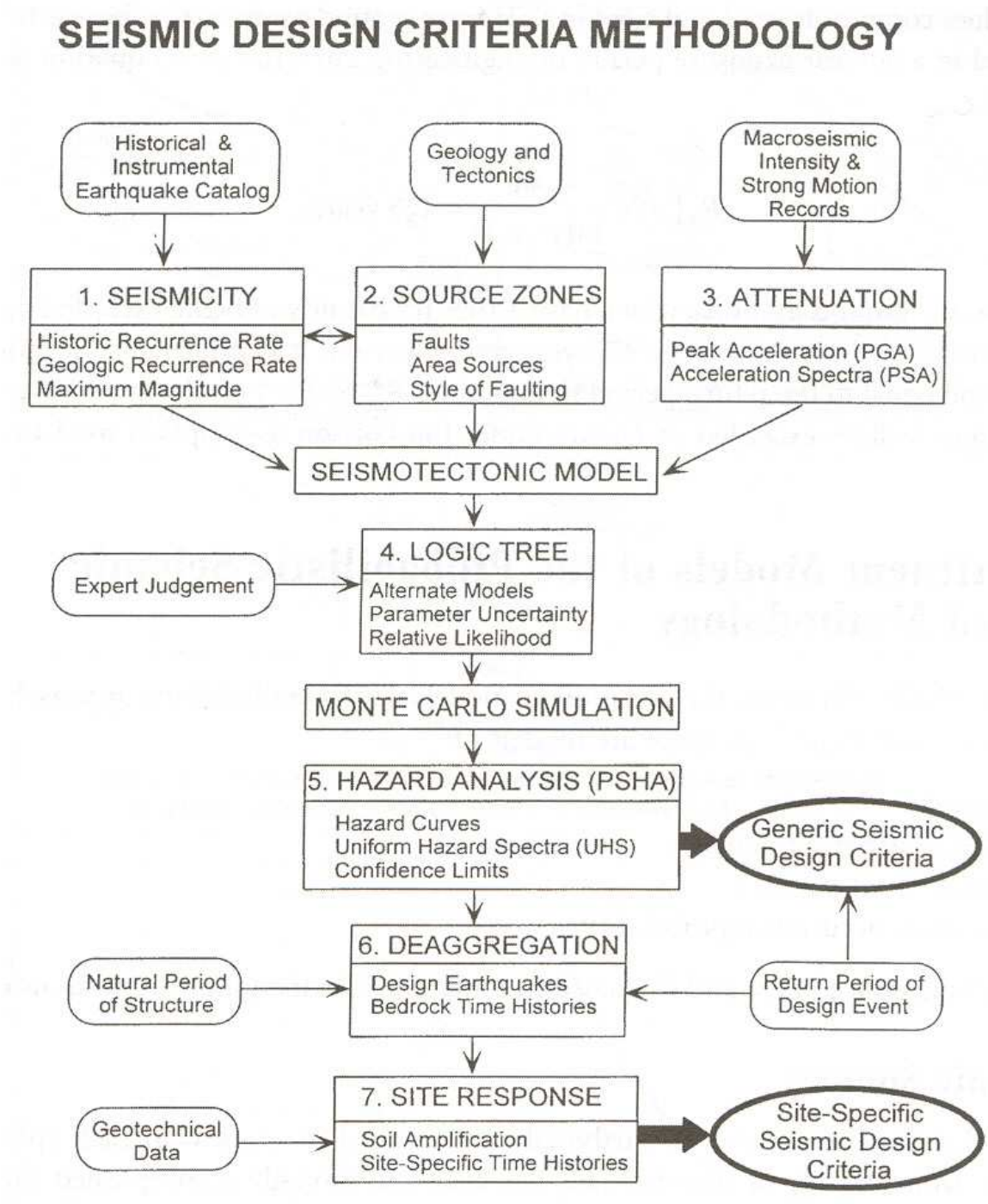

Figure 4.1 - Elements of probabilistic hazard analysis and its application in the development of seismic design criteria for structural design (Tenhaus and Campbell. In Chen and Scawthorn, 2003).

4.2 Methodology

The methodology applied follows the main trend in probabilistic seismic hazard analysis as presented by Chen and Scawthorn (2003) and McGuire (2004). Details of the approaches as applied to Icelandic seismic environment are discussed thoroughly by Ólafsson, Sigbjörnsson, Snæbjörnsson, Sólnes and Elíasson in a series of papers and reports (see the References).

A central model in seismic hazard and risk assessment is the so-called strong motion estimation equations, sometimes referred to as the attenuation scaling relationship or simply the attenuation law. It is used for prediction of strong-motion at a given site induced by a seismic event with given characteristics as discussed in the preceding chapter. By such a model it is possible to transfer the seismicity of a given seismogenic region into earthquake action required for design of structures.

The uncertainties involved in this process can be divided into two main categories, sometimes referred to as *aleatory* and *epistemic* uncertainties. The epistemic uncertainties are due to lack of knowledge required to describe the phenomenon. Obtaining new data and refining the modelling can reduce these uncertainties. Aleatory uncertainties, on the other hand, are related to the inherent unpredictability of earthquake processes. Such uncertainties cannot be reduced but are an intrinsic part of nature. It is important to be able to quantify these uncertainties correctly in the design process to ensure adequate safety and reliability of the designed structures.

The first step of the detailed computational procedure is the simulation of a parametric earthquake catalogue for the study area. The following is required:

- Definition of the seismo-tectonic model to be applied (see Chapter 2).
- Definition of the study site including uncertainty in location if required
- Definition of a study area around the study site and disregard the events outside this study area to reduce the computational effort
- Save the catalogue data for a later use
- Plot the data to indicate their geographical distribution and magnitude density

The earthquake magnitudes of the synthetic parametric earthquake catalogue are simulated as follows. For each source zone the earthquake magnitudes are assumed to follow the so-called Gutenberg-Richter magnitude law (see Chapter 2).

In the modelling it is required to select an upper boundary for the magnitudes $M_{\max}$ which should reflect the seismo-tectonic properties of each source zone. Furthermore, it is a general practice to select a lower boundary of magnitude, which usually is related to events that are so small that they do not have damaging effects on engineered structures. This lower magnitude has been taken equal to 4 in the present study for all zones, which conforms to the common practice. The upper bounds on the other hand are zone dependent (see Chapter 2).

The earthquake locations, epicentres, of the synthetic parametric earthquake catalogue are simulated as follows corresponding to each event magnitude. It is assumed that the locations of the epicentres are normally distributed with a prescribed mean location and a standard deviation. The mean location is defined along a seismic lineation, i.e. straight line, between two points, point no. i and point no. j. The statistical mean location is taken to be uniformly distributed along the seismic lineation and the individual epicentres are normally distributed around the mean location assuming in the current study that the standard deviations is isotropic, i.e. in any two perpendicular directions it is taken to be equal.

It should be underlined that it is usually required for a Monte Carlo simulation of structural response to apply a long time period. However, the length of the time period usually depends on the applications. For practical purposes it is often required to simulate at least the equivalent of 10 to 100 thousand years if annual probability values down to 10^{-4} to 10^{-5} are required.

The earthquake hazard curves are derived from the synthetic earthquake catalogue applying the strong-motion estimation models (see Chapter 3) and order statistics. Even though the simulation is carried out for a big catalogue, i.e. a catalogue covering a very long time period, the hazard curves show some random deviation from the expected smooth curve. This can be dealt with in a different way. First approach might be to treat the simulated data in a similar way as data obtained by physical measurements that is by using theory of extreme value statistics. This approach is based on application of the asymptotic extreme value distribution and may be sensitive to the data range used to derive the regression line and are, hence, depending on subjective judgements. The second alternative, a more straight forward approach, may therefore be to repeat the simulation of the hazard curve several times and then take the average value. This approach gives consistent results for the hazard values considered even after 25 simulations based on synthetic earthquake catalogue covering time period of 200 centuries. An example of the spatial distribution of the epicentres of simulated events can be seen in Figure 4.2.

However, an important question in any simulation study is: How long should the simulation series be to produce reliable results? In this context it is, however, worth noting that the variability or random behaviour observed in the computed hazard curves can partly been assigned to the simulation procedure and partly to the nature of the earthquake processes reflected in the data used to derive the strong-motion estimation equation. It is possible and desirable to reduce the fluctuations due to the numerical procedure adopted by using the above mentioned methods. Other undulations commonly seen in the uniform hazard spectra are inherent in the basic data and can only be reduced by introducing additional earthquake recordings.

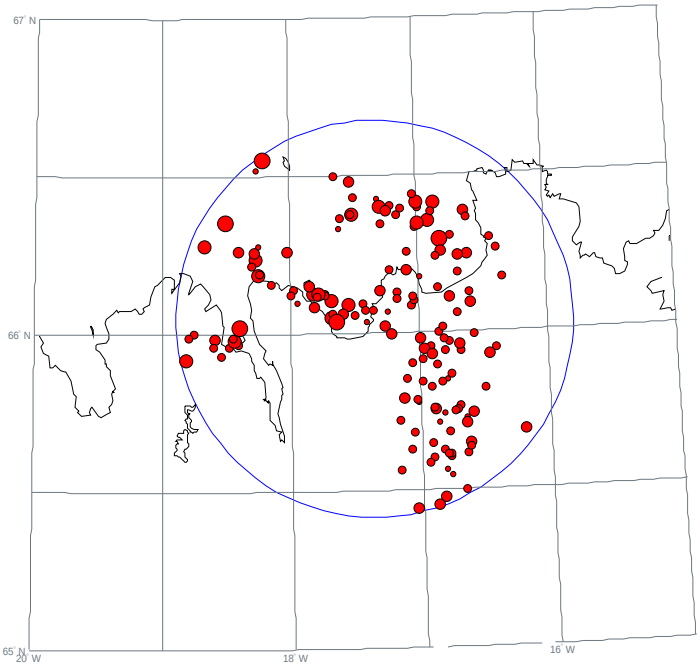

Figure 4.2 – An example of simulated parametric earthquake catalogue for North Iceland. The time period is 300 years (s = 3), study site is near Húsavík, and the radius of the study area is 70 km. The magnitude range is between 4 and 7.4, depending on the source and the simulation.

4.3 Hazard curves for peak ground acceleration

The first step in any quantitative hazard analysis may reasonably be to use an available earthquake catalogue at hand and compute the hazard curves for the desired quantities. This has been done for the horizontal peak ground acceleration applying the catalogue of Ambraseys and Sigbjörnsson (2000), which is based on instrumental data (see Chapter 2) and the strong motion estimation equations of Ambraseys et al. (2005) discussed in Chapter 3. The results are presented in Figure 4.3 for the study site assuming the site conditions being rock. It is seen that the peak ground acceleration does not exceed 20% g corresponding to mean return period equal to 100 year, i.e. annual probability of exceedance equal to 0.01. This conforms, broadly speaking, to the fact that no structural damage has been observed near the study site during the last century or so, in spite of the fact that the biggest events during that time have exceeded magnitude seven within the study area.

These short term data have been extrapolated using the methodology outlined above. The results are displayed in figure 4.4 showing the peak ground acceleration data based on a simulated catalogue and the assumed rock site conditions. The red curve reflects the hazard derived using the uncertainties in peak ground acceleration included in the applied strong-motion estimation model, while the blue curve is derived by reducing this uncertainty by factor two. For small probability there is a considerable difference between those two curves even though the deviation is only moderate for the upper part

of the curves. In the following analysis we only report curves corresponding to the red curve in figure 4.2.

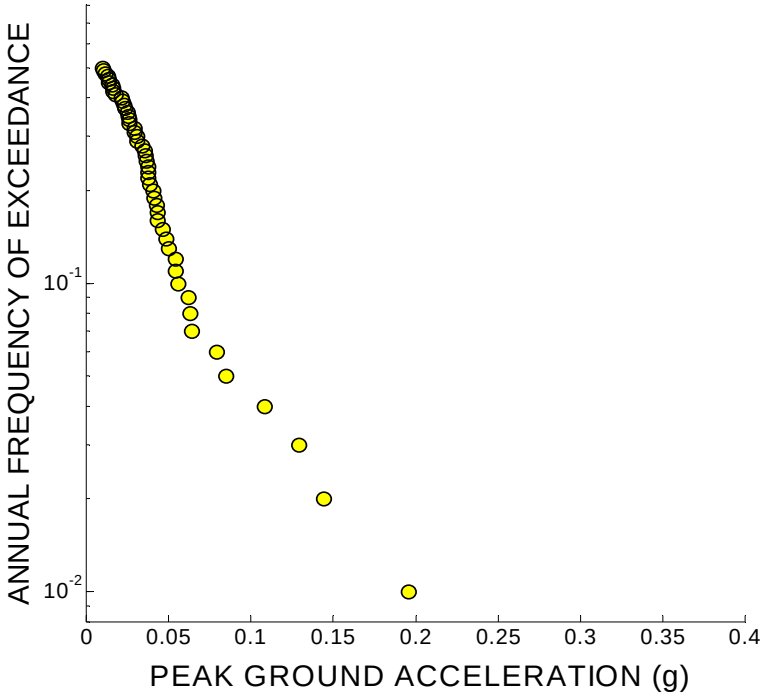

Figure 4.3– Horizontal peak ground acceleration for the study site using an instrumental earthquake catalogue and assuming rock site conditions.

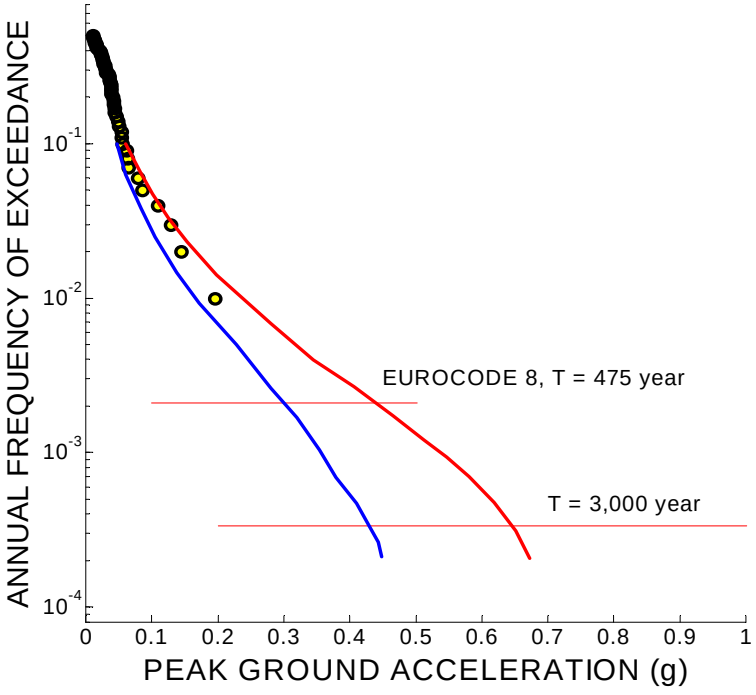

Figure 4.4 – Horizontal peak ground acceleration for the study site based on synthetic parametric earthquake catalogue and assuming rock site conditions.

The horizontal lines shown in Figure 4.4 indicate different probability levels, where especially the level corresponding to mean return period of 475 year is in accordance with Eurocode 8. The horizontal peak ground acceleration values derived from the hazard curves corresponding to some commonly used probability level are displayed in Table 4.1. The values given for mean return period equal to 475 year are in reasonable agreement with published maps for earthquake hazard in Iceland.

Similar values for the vertical peak ground acceleration are listed in Table 4.2. It is worth pointing out that the ratio between the vertical and horizontal acceleration is about 60% for the mean return period in the tables, except for the longest period reported. It is also noted that this ratio approaches 1 as the mean return period becomes very long, say, 10,000 year or more.

Table 4.1 - Horizontal peak ground acceleration (PGA) derived from the hazard curves.

Reference	*Mean return period* (year)	*Annual probability of exceedance*	*Probability of exceedance in 50 years*	*Simulated horizontal PGA* (g)
	95	1.05%	40.92	0.21
	144	0.69%	29.3%	0.26
EUROCODE 8	475	0.21%	10.0%	0.44
	1,000	0.10%	4.88%	0.56
	3,000	0.033%	1.65%	0.65

Table 4.1 - Vertical peak ground acceleration (PGA) derived from the hazard curves.

Reference	*Mean return period* (year)	*Annual probability of exceedance*	*Probability of exceedance in 50 years*	*Simulated vertical PGA* (g)
	95	1.05%	40.92	0.13
	144	0.69%	29.3%	0.15
EUROCODE 8	475	0.21%	10.0%	0.27
	1,000	0.10%	4.88%	0.34
	3,000	0.033%	1.65%	0.53

4.4 Uniform hazard spectrum for linear elastic response

The uniform hazard spectrum is derived in a similar manner as the above presented peak ground acceleration values in Tables 4.1 and 4.2. The starting point is a synthetic parametric earthquake catalogue. In general it enhances the accuracy of the estimation if more than one catalogue is applied. Then the hazard curves for the spectral ordinates are derived using the strong-motion estimation models presented in Chapter 3. The results are in principle reflected in Figure 4.5 below.

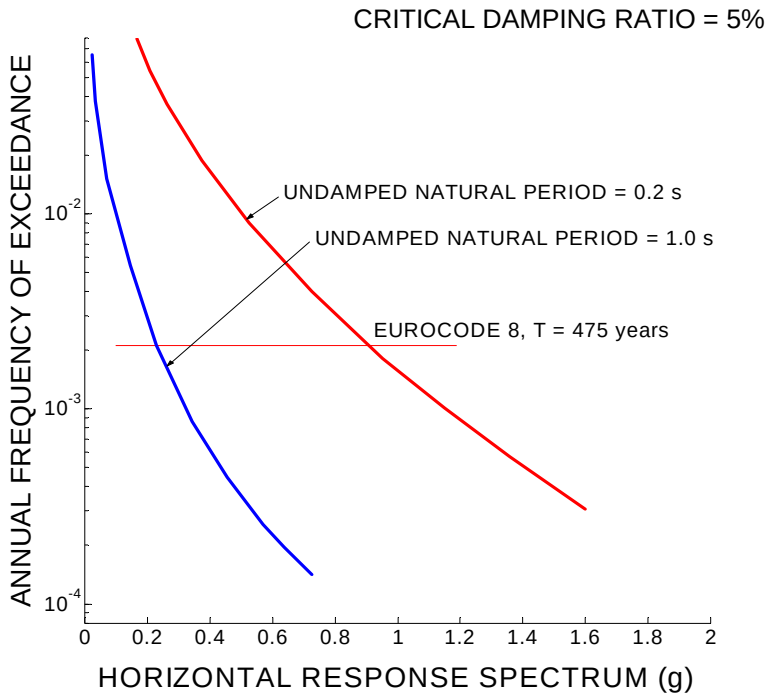

Figure 4.5 – Horizontal response spectrum ordinates for the study site based on synthetic parametric earthquake catalogue and assuming rock site conditions. Two different undamped natural periods are included, respectively, 0.2 s (red curve, and 1.0 s (blue curve). The critical damping ratio is 5% in both cases.

The uniform hazard spectra are then obtained from the hazard curves covering undamped natural periods logarithmically spaced in the range 0.06 to 2.0 s. In all cases the critical damping ratio is taken equal to 5% of the critical value. The results are showed in Figure 4.6 and 4.7, respectively, for the horizontal and vertical action from. Corresponding values are given in Table 4.3 and 4.4.

To facilitate the comparison of the uniform hazard spectra with standardise codified spectra a normalisation is performed using the peak ground acceleration as a reference value. This process gives the curves presented in Figure 4.8 and 4.9 below.

It is seen that the variation of the normalised spectra for the different mean return period is not very great. This supports the commonly accepted simplification to adopt only one curve to describe the normalised spectrum. Especially this appears to be reasonable for the vertical action.

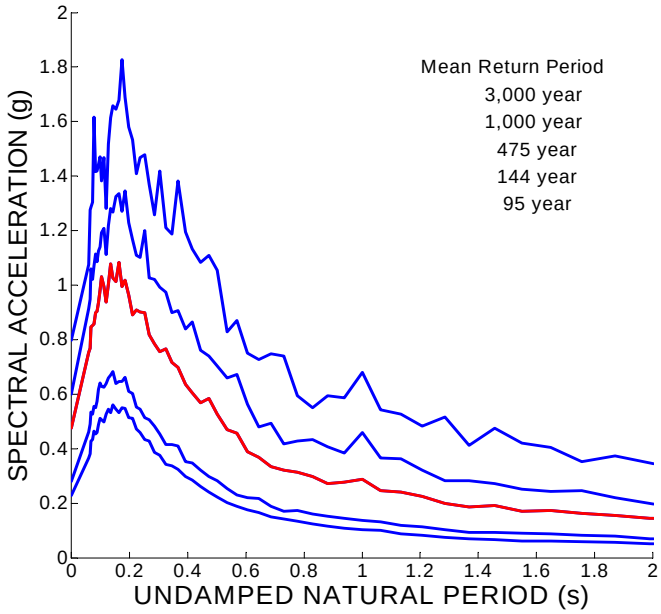

Figure 4.6 – Horizontal earthquake response spectra for linear elastic systems under uniform hazard. Critical damping ratio is equal to 5%. Site conditions are rock.

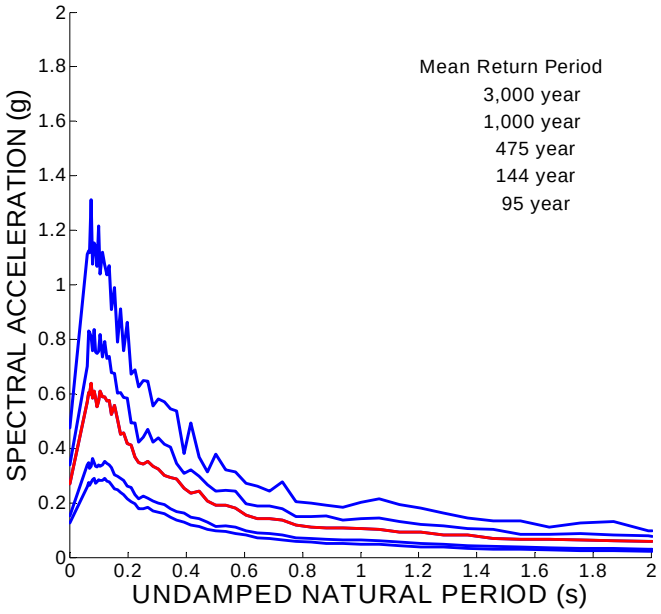

Figure 4.7 – Vertical earthquake response spectra for linear elastic systems under uniform hazard. Critical damping ratio is equal to 5%. Site conditions are rock.

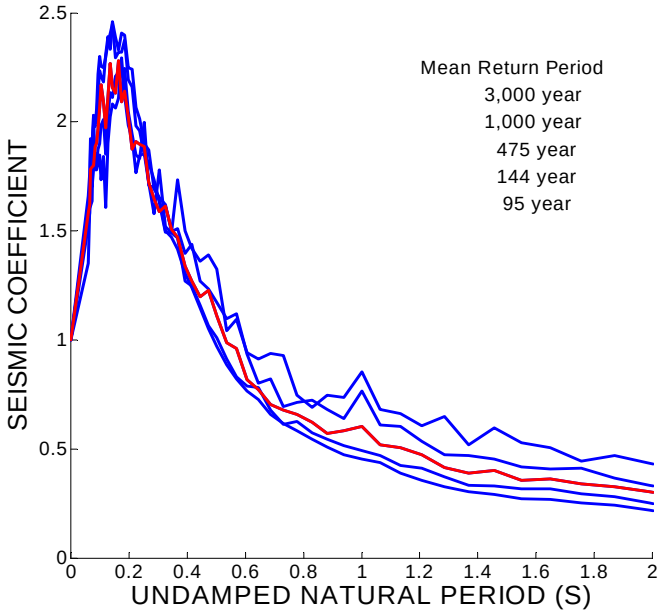

Figure 4.8 – Normalised horizontal earthquake response spectra for linear elastic systems under uniform hazard. Critical damping ratio is equal to 5%. Site conditions are rock.

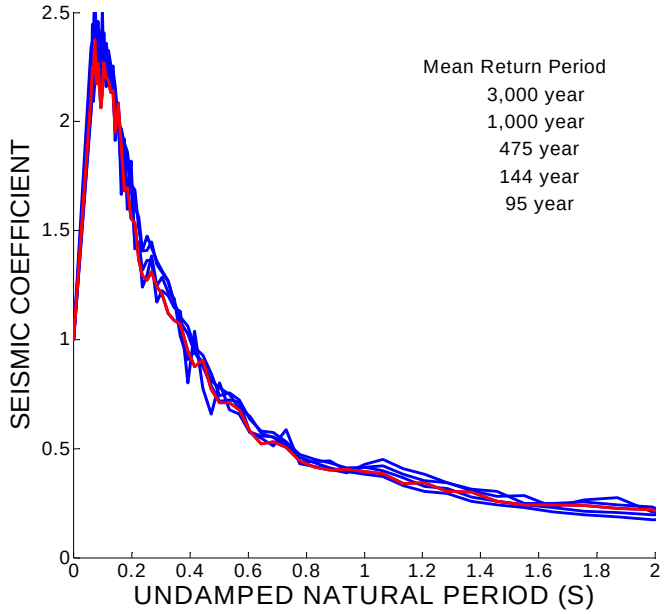

Figure 4.9 – Normalised vertical earthquake response spectra for linear elastic systems under uniform hazard. Critical damping ratio is equal to 5%. Site conditions are rock.

Table 4.3 – Horizontal spectral ordinates. T is the mean return period corresponding to the probabilities listed in Table 4.1 and 4.2. Critical damping ratio is equal to 5%. Site conditions are rock.

Natural Period	***Horizontal Spectral ordinates*** (g)			
(s)	T = 95 year	T = 144 year	T = 475 year	T = 1000 year
0.000E+00	2.114E-01	2.578E-01	4.403E-01	5.559E-01
6.000E-02	3.389E-01	4.280E-01	6.966E-01	8.458E-01
6.387E-02	3.537E-01	4.549E-01	7.128E-01	8.786E-01
6.799E-02	3.961E-01	4.960E-01	7.845E-01	9.803E-01
7.238E-02	4.016E-01	4.880E-01	7.898E-01	9.457E-01
7.705E-02	4.292E-01	5.135E-01	7.924E-01	9.908E-01
8.202E-02	4.207E-01	5.097E-01	8.314E-01	1.031E+00
8.731E-02	4.247E-01	5.309E-01	8.373E-01	1.006E+00
9.295E-02	4.513E-01	5.716E-01	8.662E-01	1.041E+00
9.894E-02	4.727E-01	5.928E-01	9.100E-01	1.056E+00
1.053E-01	4.672E-01	5.809E-01	9.555E-01	1.103E+00
1.121E-01	4.616E-01	5.796E-01	9.215E-01	1.118E+00
1.194E-01	4.883E-01	5.923E-01	8.685E-01	1.030E+00
1.271E-01	5.052E-01	6.096E-01	9.295E-01	1.128E+00
1.353E-01	4.931E-01	6.193E-01	9.978E-01	1.187E+00
1.440E-01	5.201E-01	6.314E-01	9.491E-01	1.174E+00
1.533E-01	5.048E-01	5.914E-01	9.382E-01	1.228E+00
1.632E-01	4.923E-01	5.979E-01	1.004E+00	1.237E+00
1.737E-01	5.087E-01	5.981E-01	9.216E-01	1.177E+00
1.849E-01	5.067E-01	6.124E-01	9.420E-01	1.247E+00
1.968E-01	4.756E-01	5.648E-01	8.915E-01	1.138E+00
2.095E-01	4.737E-01	5.566E-01	8.257E-01	1.080E+00
2.230E-01	4.367E-01	5.108E-01	8.408E-01	1.027E+00
2.374E-01	4.255E-01	5.049E-01	8.347E-01	1.019E+00
2.527E-01	4.021E-01	4.761E-01	8.312E-01	1.111E+00
2.691E-01	3.957E-01	4.676E-01	7.576E-01	9.493E-01
2.864E-01	3.577E-01	4.467E-01	7.251E-01	9.442E-01
3.049E-01	3.484E-01	4.206E-01	6.995E-01	9.198E-01
3.246E-01	3.173E-01	3.851E-01	7.099E-01	9.017E-01
3.455E-01	3.109E-01	3.841E-01	6.629E-01	8.325E-01
3.678E-01	2.993E-01	3.787E-01	6.476E-01	8.401E-01
3.915E-01	2.758E-01	3.271E-01	5.883E-01	7.769E-01
4.168E-01	2.626E-01	3.212E-01	5.590E-01	7.999E-01
4.437E-01	2.424E-01	2.984E-01	5.271E-01	7.048E-01
4.723E-01	2.224E-01	2.748E-01	5.401E-01	6.855E-01
5.028E-01	2.052E-01	2.605E-01	4.882E-01	6.508E-01
5.352E-01	1.876E-01	2.351E-01	4.346E-01	6.097E-01
5.697E-01	1.735E-01	2.139E-01	4.226E-01	6.231E-01
6.065E-01	1.622E-01	2.030E-01	3.605E-01	5.202E-01
6.456E-01	1.538E-01	2.013E-01	3.401E-01	4.453E-01
6.873E-01	1.392E-01	1.747E-01	3.099E-01	4.563E-01
7.316E-01	1.305E-01	1.576E-01	2.979E-01	3.862E-01
7.788E-01	1.236E-01	1.611E-01	2.896E-01	3.961E-01
8.291E-01	1.155E-01	1.477E-01	2.747E-01	4.020E-01
8.826E-01	1.077E-01	1.404E-01	2.512E-01	3.779E-01
9.395E-01	1.001E-01	1.329E-01	2.568E-01	3.546E-01
1.000E+00	9.583E-02	1.272E-01	2.651E-01	4.260E-01
1.065E+00	9.278E-02	1.213E-01	2.286E-01	3.385E-01
1.133E+00	8.186E-02	1.096E-01	2.233E-01	3.361E-01
1.206E+00	7.554E-02	1.058E-01	2.077E-01	2.968E-01
1.284E+00	6.938E-02	9.555E-02	1.831E-01	2.624E-01
1.367E+00	6.438E-02	8.557E-02	1.712E-01	2.610E-01
1.455E+00	6.119E-02	8.515E-02	1.763E-01	2.521E-01
1.549E+00	5.717E-02	8.203E-02	1.571E-01	2.317E-01
1.649E+00	5.649E-02	8.131E-02	1.592E-01	2.263E-01
1.756E+00	5.339E-02	7.573E-02	1.499E-01	2.284E-01
1.869E+00	5.136E-02	7.233E-02	1.439E-01	2.031E-01
1.990E+00	4.629E-02	6.482E-02	1.340E-01	1.849E-01
2.118E+00	4.250E-02	5.889E-02	1.186E-01	1.625E-01
2.255E+00	3.890E-02	5.554E-02	1.131E-01	1.693E-01

Table 4.4 – Vertical spectral ordinates. T is the mean return period corresponding to the probabilities listed in Table 4.1 and 4.2. Critical damping ratio is equal to 5%. Site conditions are rock.

Natural Period	***Horizontal Spectral ordinates*** (g)			
(s)	T = 95 year	T = 144 year	T = 475 year	T = 1000 year
0.000E+00	1.263E-01	1.522E-01	2.685E-01	3.400E-01
6.000E-02	2.581E-01	3.387E-01	5.697E-01	7.010E-01
6.387E-02	2.752E-01	3.466E-01	6.048E-01	8.320E-01
6.799E-02	2.643E-01	3.267E-01	5.958E-01	8.262E-01
7.238E-02	2.755E-01	3.351E-01	6.377E-01	8.110E-01
7.705E-02	2.856E-01	3.639E-01	5.835E-01	7.572E-01
8.202E-02	2.899E-01	3.475E-01	6.086E-01	8.360E-01
8.731E-02	2.725E-01	3.343E-01	5.851E-01	7.517E-01
9.295E-02	2.764E-01	3.324E-01	5.534E-01	7.476E-01
9.894E-02	2.836E-01	3.387E-01	5.743E-01	7.563E-01
1.053E-01	2.829E-01	3.329E-01	6.094E-01	8.188E-01
1.121E-01	2.814E-01	3.402E-01	5.901E-01	7.348E-01
1.194E-01	2.888E-01	3.537E-01	5.882E-01	7.914E-01
1.271E-01	2.808E-01	3.440E-01	5.726E-01	7.289E-01
1.353E-01	2.776E-01	3.406E-01	5.754E-01	7.367E-01
1.440E-01	2.658E-01	3.286E-01	5.240E-01	6.772E-01
1.533E-01	2.500E-01	3.042E-01	5.588E-01	6.757E-01
1.632E-01	2.487E-01	2.988E-01	5.062E-01	6.018E-01
1.737E-01	2.374E-01	2.891E-01	4.519E-01	6.041E-01
1.849E-01	2.298E-01	2.834E-01	4.558E-01	5.868E-01
1.968E-01	2.133E-01	2.604E-01	4.174E-01	5.832E-01
2.095E-01	2.032E-01	2.565E-01	4.117E-01	4.924E-01
2.230E-01	1.974E-01	2.300E-01	3.674E-01	4.919E-01
2.374E-01	1.778E-01	2.144E-01	3.465E-01	4.216E-01
2.527E-01	1.782E-01	2.243E-01	3.420E-01	4.400E-01
2.691E-01	1.827E-01	2.164E-01	3.522E-01	4.699E-01
2.864E-01	1.696E-01	2.069E-01	3.334E-01	4.235E-01
3.049E-01	1.654E-01	2.001E-01	3.242E-01	4.375E-01
3.246E-01	1.598E-01	1.931E-01	3.010E-01	4.139E-01
3.455E-01	1.476E-01	1.780E-01	2.917E-01	4.040E-01
3.678E-01	1.365E-01	1.679E-01	2.874E-01	3.454E-01
3.915E-01	1.294E-01	1.613E-01	2.544E-01	3.086E-01
4.168E-01	1.191E-01	1.468E-01	2.355E-01	3.214E-01
4.437E-01	1.133E-01	1.412E-01	2.429E-01	2.975E-01
4.723E-01	1.025E-01	1.282E-01	2.070E-01	2.678E-01
5.028E-01	9.835E-02	1.132E-01	1.903E-01	2.442E-01
5.352E-01	9.453E-02	1.150E-01	1.906E-01	2.459E-01
5.697E-01	8.645E-02	1.103E-01	1.818E-01	2.426E-01
6.065E-01	8.209E-02	9.654E-02	1.558E-01	1.964E-01
6.456E-01	7.208E-02	8.847E-02	1.405E-01	1.892E-01
6.873E-01	6.951E-02	8.756E-02	1.427E-01	1.888E-01
7.316E-01	6.457E-02	8.068E-02	1.360E-01	1.786E-01
7.788E-01	5.826E-02	7.207E-02	1.194E-01	1.495E-01
8.291E-01	5.492E-02	6.866E-02	1.112E-01	1.498E-01
8.826E-01	5.196E-02	6.603E-02	1.082E-01	1.511E-01
9.395E-01	4.993E-02	6.276E-02	1.085E-01	1.355E-01
1.000E+00	4.817E-02	6.327E-02	1.064E-01	1.414E-01
1.065E+00	4.713E-02	6.041E-02	1.033E-01	1.437E-01
1.133E+00	4.176E-02	5.555E-02	9.104E-02	1.303E-01
1.206E+00	3.823E-02	4.971E-02	9.250E-02	1.198E-01
1.284E+00	3.698E-02	4.811E-02	8.170E-02	1.166E-01
1.367E+00	3.258E-02	4.237E-02	8.078E-02	1.062E-01
1.455E+00	3.078E-02	3.939E-02	6.980E-02	1.033E-01
1.549E+00	2.875E-02	3.702E-02	6.531E-02	8.479E-02
1.649E+00	2.642E-02	3.503E-02	6.518E-02	8.425E-02
1.756E+00	2.483E-02	3.219E-02	6.402E-02	8.646E-02
1.869E+00	2.376E-02	3.165E-02	6.061E-02	8.277E-02
1.990E+00	2.208E-02	3.013E-02	5.849E-02	7.863E-02
2.118E+00	1.916E-02	2.638E-02	4.809E-02	6.410E-02
2.255E+00	1.971E-02	2.645E-02	4.958E-02	6.824E-02

In our presentation so far only linear elastic systems have been considered, which is not entirely satisfactory for design. The reason for this is in the first place that engineered structures usually do not behave strictly linearly and in the second place it is economically feasible to utilise the inelastic structural behaviour to dissipate the earthquake-induced wave energy. This is commonly achieved in codes introducing so-called structural behaviour factor which is used to reduce the strength demand. The reduction of strength, on the other hand, increases the displacement demand and on the same time the ductility demand. Unfortunately, the structural behaviour factors do not depend only on the structural property as such but depends also on the properties of the earthquake action, like the spectral composition of accelerograms and duration characteristics to mention two important quantities. In next section the properties of inelastic behaviour are explored and the structural behaviour factor is assessed.

4.5 Uniform hazard spectrum for inelastic response

The inelastic spectral acceleration response was derived using the data from the earthquakes listed in Table 4.5 (Ambraseys et al., 2004). The faulting mechanisms of the earthquakes were all classified as being strike-slip and the site characteristics of the stations were classified as rock. The data originates from eight earthquakes and consist of 48 records, all together 144 time series. Majority of the records is from Iceland. However, they have been augmented with data from the European strong-motion databank.

Based on this dataset two strong-motion estimation equations have been constructed for elasto-plastic systems with undamped natural period equal to 0.2 s and 1.0 s, respectively, both with critical damping ratio equal to 5% and ductility ratio equal to 2. These strong-motion curves are shown in Figure 4.10 along with comparable curves for linear elastic system according to Ambraseys et al. (2005) assuming the earthquake magnitude equal to 6.5. It is seen that the linear elastic system response is significantly bigger than the inelastic response concerning strength demand, which is not necessarily the case for the displacement demand. This is illustrated on Figure 4.10 showing the so-called structural behaviour factor.

The structural behaviour factor is defined as the quantity required for transforming the linear elastic response spectral acceleration into an inelastic demand. This can be expressed in a simplified way as follows:

$$S_{inelastic}(T,\lambda,\mu) = S_a(T,\lambda)/k(\mu,T) \qquad (4.1)$$

Here, $S_{inelastic}$ is the inelastic strength spectrum for the elasto-plastic system, S_a is acceleration spectrum for the linear elastic system, k is the structural behaviour factor, T is the undamped natural period of the linear elastic system, which is taken equal to the initial small amplitude undamped natural period of the inelastic system, λ is the critical damping ratio and μ is the ductility ratio.

Table 4.5 – Earthquake data used for inelastic analysis (Ambraseys et al., 2004). The faulting mechanism of the earthquakes is strike-slip and the site conditions of the stations are rock. Abbreviations used for country names are: AR (Armenia), GR (Greece), IS (Iceland), IT (Italy), SL (Slovenia), TU (Turkey).

Date	**Time**	**Country**	M_w	**Station**	**Distance** (km)
26.8.1983	12:52:09	GR	5.20	Ouranoupolis-Seismograph Station	15
26.8.1983	12:52:09	GR	5.20	Poligiros-Prefecture	42
16.12.1990	15:45:51	AR	5.48	Akhalkalaki	20
16.12.1990	15:45:51	AR	5.48	Toros	51
16.12.1990	15:45:51	AR	5.48	Stepanavan	70
16.12.1990	15:45:51	AR	5.48	Spitak-Karadzor	77
26.4.1997	22:18:34	GR	5.02	Kyparrisia-Agriculture Bank	26
16.10.1997	12:00:31	IT	4.39	Colfiorito-Casermette	1
16.10.1997	12:00:31	IT	4.39	Nocera Umbra-Biscontini	10
16.10.1997	12:00:31	IT	4.39	Nocera Umbra	12
12.4.1998	10:55:33	SL	5.70	Cerknica	88
12.4.1998	10:55:33	SL	5.70	Sleme	104
4.6.1998	21:36:54	IS	5.45	Hveragerdi-Church	6
4.6.1998	21:36:54	IS	5.45	Irafoss-Hydroelectric Power Station	15
4.6.1998	21:36:54	IS	5.45	Selfoss-Hospital	18
4.6.1998	21:36:54	IS	5.45	Oseyrarbru	18
4.6.1998	21:36:54	IS	5.45	Reykjavik-Heidmork	23
4.6.1998	21:36:54	IS	5.45	Reykjavik-Foldaskoli	27
4.6.1998	21:36:54	IS	5.45	Reykjavik-HusVerslunarinnar	32
17.8.1999	00:01:40	TU	7.64	Izmit-Meteoroloji	9
17.8.1999	00:01:40	TU	7.64	Gebze-Tubitak Marmara Arastirma Merkezi	47
17.8.1999	00:01:40	TU	7.64	Yapi-Kredi Plaza Levent	92
17.8.1999	00:01:40	TU	7.64	Istanbul-Maslak	93
17.8.1999	00:01:40	TU	7.64	Tokat-DSI Misafirhanesi	558
17.6.2000	15:40:41	IS	6.57	Flagbjarnarholt	5
17.6.2000	15:40:41	IS	6.57	Minni-Nupur	13
17.6.2000	15:40:41	IS	6.57	Thjorsarbru	15
17.6.2000	15:40:41	IS	6.57	Selfoss-Hospital	31
17.6.2000	15:40:41	IS	6.57	Selfoss-City	32
17.6.2000	15:40:41	IS	6.57	Irafoss-Hydroelectric Power Station	34
17.6.2000	15:40:41	IS	6.57	Ljosafoss-Hydroelectric Power Station	35
17.6.2000	15:40:41	IS	6.57	Hveragerdi-Retirement House	41
17.6.2000	15:40:41	IS	6.57	Hveragerdi-Church	41
17.6.2000	15:40:41	IS	6.57	Sultartanga-Hydroelectric Power Station	42
17.6.2000	15:40:41	IS	6.57	Hrauneyjafoss-Hydroelectric Power Station	61
17.6.2000	15:40:41	IS	6.57	Reykjavik-Heidmork	70
17.6.2000	15:40:41	IS	6.57	Reykjavik-Foldaskoli	72
17.6.2000	15:40:41	IS	6.57	Reykjavik-Hus Verslunarinnar	78
21.6.2000	00:51:48	IS	6.49	Thjorsarbru	5
21.6.2000	00:51:48	IS	6.49	Thjorsartun	6
21.6.2000	00:51:48	IS	6.49	Selfoss-Hospital	14
21.6.2000	00:51:48	IS	6.49	Selfoss-City Hall	15
21.6.2000	00:51:48	IS	6.49	Irafoss-Hydroelectric Power Station	20
21.6.2000	00:51:48	IS	6.49	Ljosafoss-Hydroelectric Power Station	20
21.6.2000	00:51:48	IS	6.49	Flagbjarnarholt	22
21.6.2000	00:51:48	IS	6.49	Hveragerdi-Church	24
21.6.2000	00:51:48	IS	6.49	Hveragerdi-Retirement House	24
21.6.2000	00:51:48	IS	6.49	Minni-Nupur	28
21.6.2000	00:51:48	IS	6.49	Reykjavik-Heidmork (Jadar)	53

It follows that both the spectra and the structural behaviour factor must be function of epicentral distance (site-to-source distance), site conditions, faulting mechanism and the selected hazard level. Figure 4.11 shows that the structural behaviour factor increases with increasing distance to source. Furthermore, almost in the entire range the structural behaviour factor is significantly bigger for the stiff system considered than the flexible system.

The hazard curve of the horizontal acceleration response ordinates for elasto-plastic system at the study site based on a synthetic parametric earthquake catalogue and assuming rock site conditions is shown in Figure 4.12. Undamped natural period is 0.2 s, the critical damping ratio is 5% and the ductility ratio is equal to 2. Also in this case we see a significant reduction of the strength demand compared to the linear elastic system. The structural behaviour factors have been computed for different probability levels and the results are displayed in Figure 4.13. It is seen that for the system considered that the structural behaviour factor is almost 3 corresponding to 475 year mean return period.

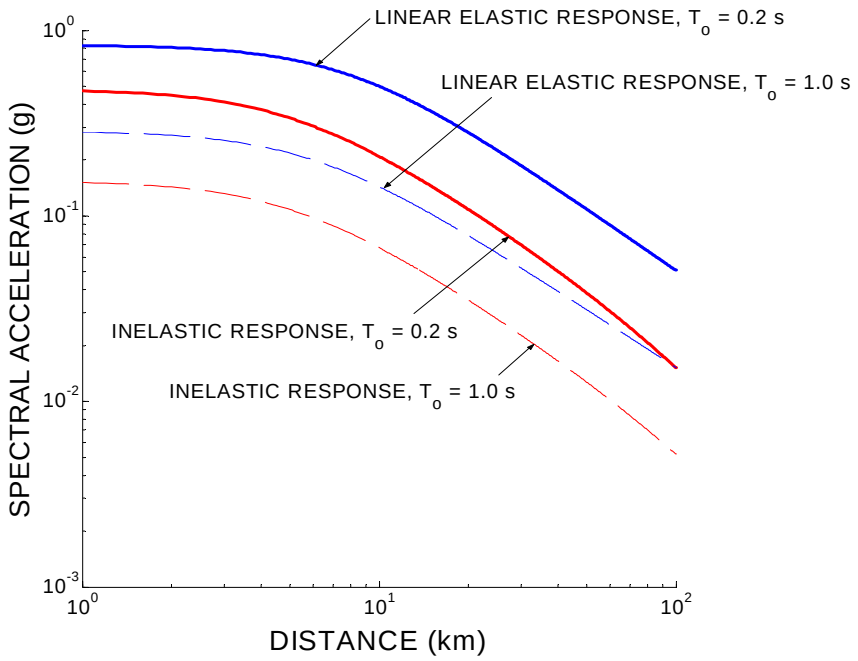

Figure 4.10 – Horizontal spectral acceleration of linear elastic systems and the strength of inelastic elasto-plastic systems as a function of distance to source. The response is induced by magnitude 6.5 earthquake.

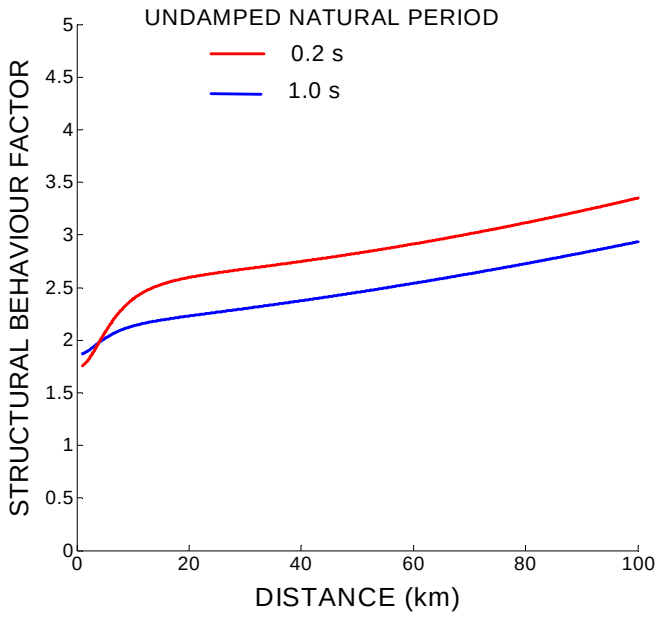

Figure 4.11 – Structural behaviour factor for horizontal response relating the spectral acceleration of linear elastic systems to the strength of inelastic elasto-plastic systems expressed as a function of distance to source. The response is induced by a magnitude 6.5 earthquake. Critical damping ration is equal to 5% and ductility ratio is equal to 2.

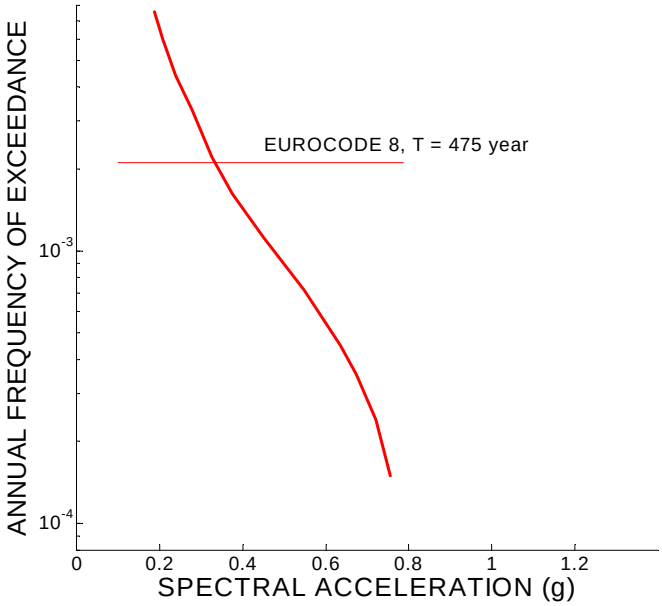

Figure 4.12 – Horizontal response spectrum ordinates for elasto-plastic system at the study site based on synthetic parametric earthquake catalogue and assuming rock site conditions. Undamped natural period is 0.2 s, the critical damping ratio is 5% and the ductility ratio is assumed equal to 2.

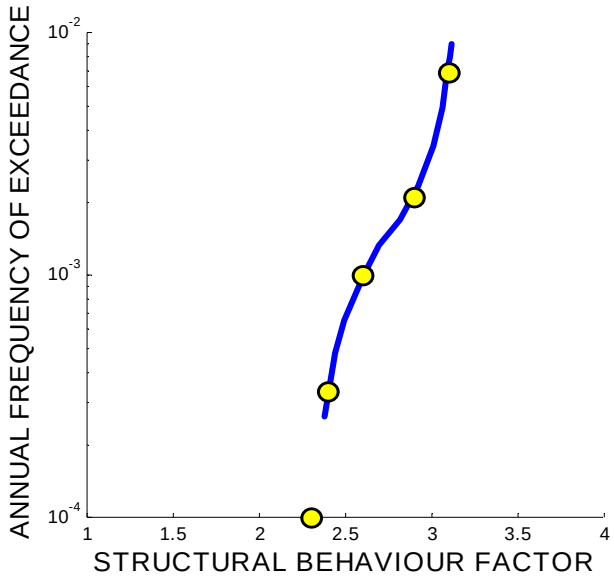

Figure 4.13 – Structural behaviour factor for horizontal response acceleration ordinates for elasto-plastic system at the study site based on synthetic parametric earthquake catalogue and assuming rock site conditions. Undamped natural period is 0.2 s, the critical damping ratio is 5% and the ductility ratio is assumed equal to 2.

5. SUGGESTED DESIGN SPECIFICATIONS

5.1 Definition of earthquake action

It is recommended that the following different earthquake actions should be considered in design, i.e. an Operating Base Earthquake for no damage and undisturbed plant operation, a Maximum Design Earthquake for life safety and limited damage and a Maximum Credible Earthquake for collapse prevention checking. Theses actions are defined as follows:

The Operating Base Earthquake (OBE) is defined as an earthquake that can reasonably be expected to occur within the service life of the project, that is, within a 50% probability of exceedence during service life. This corresponds to a return period of 144 years for a project with a service life of 100 years and a return period of 95 years for a project service life of 50 years. The associated performance requirement is that the project functions with little or no damage, and without interruption of function. The purpose of the OBE is to protect against economic losses from damage or loss of service; therefore, alternative choices of return period for the OBE may be based on economic considerations.

The Maximum Design Earthquake (MDE) is defined ad the maximum level of ground motion for which a structure is designed or evaluated. The associated performance requirement is that the project performs without catastrophic failure although severe damage or economic loss may be tolerated.

The Maximum Credible Earthquake (MCE) is defined as the greatest earthquake that can reasonably be expected to be generated by a specific source on the basis of seismological and geological evidence.

For critical structures, especially in low seismicity zones, it is sometimes required that the MDE be set equal to the MCE. Structures are considered critical if their failure during or following an earthquake could result in loss of life. However, generally the MDE is selected as a less severe event than the MCE, which provides for an economical design meeting specified safety standards. The MDE is chosen based upon an appropriate probability of exceedence of ground motions during the design life of the structure, such as 10 percent probability of exceedence in 50 to 100 years. This corresponds to a return period of 475 and 950 years, for a project with a service life of 50 and 100 years, respectively.

It is recommended that an event corresponding to mean return period equal to 95 year is defined as an operating base earthquake, an event defined for 475 year mean return period as maximum design earthquake and an event corresponding to 1000 year mean return period as maximum credible earthquake.

Based on probabilistic hazard analysis it is recommended that the PGA-values summarised in Table 4.1 shall be used as the basic quantities for the definition of uniform hazard spectra for horizontal action and the PGA-values summarised in Table 4.2

shall be used as the basic quantities for the definition of uniform hazard spectra for vertical action.

Simulated uniform hazard spectra for horizontal action are given in Figure 4.3 and the corresponding seismic coefficient in Figure 4.5. Spectral ordinates of the type commonly used in engineering design, given in the terms of the seismic coefficient, are given by the following expression:

$$S_a = \begin{cases} PGA_{horizontal} \times \left(1 + \dfrac{T}{0.1} \times (2.3 - 1)\right) & 0\,s \le T < 0.1\,s \\ PGA_{horizontal} \times 2.3 & 0.1\,s \le T < 0.25\,s \\ PGA_{horizontal} \times 2.3 \left(\dfrac{0.25}{T}\right)^{5/6} & 0.25\,s \le T < 2\,s \end{cases} \qquad (5.1)$$

Here, $PGA_{horizontal}$ is the horizontal peak ground acceleration (see Table 1), T is the undamped natural period in seconds (s) and the critical damping ratio is taken as 5%. This simplified expression for the uniform hazard spectrum is plotted in Figure 5.1.

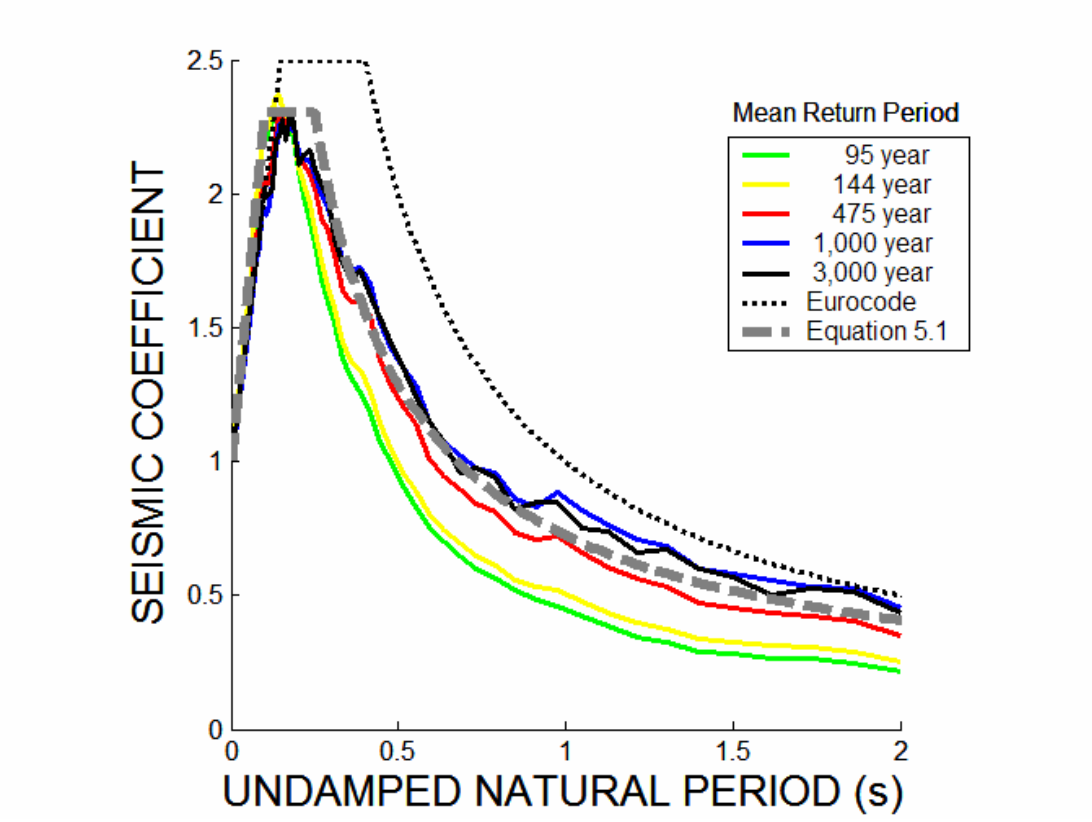

Figure 5.1 – Suggested seismic coefficients (normalised spectral acceleration ordinates) for horizontal earthquake action (red curve) plotted along with simulated data (see text and Figure 2). Critical damping ratio is equal to 5%. Rock conditions are assumed.

A simulated uniform hazard spectra for vertical action are given in Figure 4.4 and the corresponding seismic coefficient in Figure 4.6. Similar to the horizontal action specified above, spectral ordinates of the vertical action, given in the terms of the seismic coefficient, are given by the following expression:

$$S_a = \begin{cases} PGA_{vertical} \times \left(1 + \dfrac{T}{0.05}(2.5-1)\right) & 0\,s \le T < 0.05\,s \\ PGA_{vertical} \times 2.5 & 0.05\,s \le T < 0.13\,s \\ PGA_{vertical} \times 2.5\left(\dfrac{0.13}{T}\right)^{7/8} & 0.13\,s \le T < 2\,s \end{cases} \qquad (5.2)$$

Here, $PGA_{vertical}$ is the vertical peak ground acceleration (see Table 2), T is the undamped natural period in seconds (s) and the critical damping ratio is taken as 5%. This simplified expression for the uniform hazard spectrum is plotted in Figure 5.2.

The horizontal and vertical action described above can be treated as statistically independent. Hence, the horizontal and vertical acceleration can be regarded as uncorrelated.

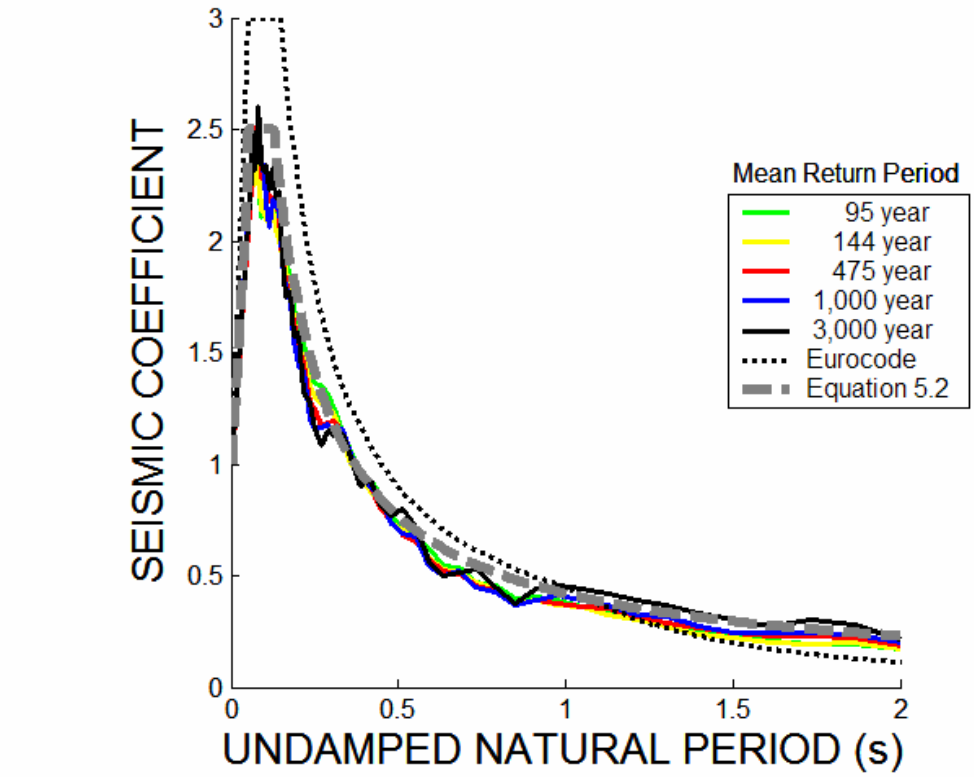

Figure 5.2 – Suggested seismic coefficients (normalised spectral acceleration ordinates) for vertical earthquake action (red curve) plotted along with simulated data (see text and Figure 5). Critical damping ratio is equal to 5%. Rock conditions are assumed.

Comment on the application of the design response spectra

The response spectra for horizontal and vertical action have been defined for three natural period regimes. It is appropriate to point out, that spectral shapes for the lowest natural period regimes may be suitable for an OBE event. However, it is recommended that for an MDE or an MCE event the second spectral regime is applied for structures of low natural period. During an MDE and MCE events substantial deterioration of structures is generally predicted and consequently the natural period may increase resulting in an un-conservative design if the first part of the response spectra is applied.

Comment on the inelastic effects

It is seen that the derived linear elastic response spectrum has distinct features that are different from what is seen in the case of the normalised standard spectrum in Eurocode 8 referred to the guideline table values.[2] The constant acceleration part of the spectrum is slightly lower and narrower than anticipated in the guidelines. The reason for this is that the Icelandic seismic environment only contains small to moderately sized earthquakes with very few events exceeding magnitude seven. This fact has also effects on the inelastic response which tends to be significantly smaller than anticipated from the experience of big earthquakes. The result is that the structural behaviour factor for Icelandic seismic environments is generally bigger than the guideline values given in Eurocode 8. Based on this finding the linear elastic response spectrum for mean return period equal to 475 year can be used with confidence combined with a structural behaviour factor equal to 2.9 corresponding to 0.2 s undamped natural period, 5% critical damping ratio and ductility ratio equal to 2 assuming rock site conditions. Hence the maximum base shear for this structure would be:

$$\begin{aligned} F_{\max}\left(T_o = 0.2; \mu = 2; \lambda = 5\%; rock\ site\right) \\ = m \times PGA \times S\left(T_o, \lambda | site\right) / k\left(\mu | T_o, \lambda, site\right) \\ = m \times 0.44 \times 2.25 / 2.9 = 0.34 \times m \end{aligned} \qquad (5.3)$$

Here, m is the structural mass, S refers to the normalised spectral ordinates (see Figure 5.1 and 5.2) and k is the structural behaviour factor (see Figure 4.12). It should be noted that for other return periods than 475 the results would be different. Furthermore, natural period, damping and ductility ratio as well as site conditions may lead to different values. None the less, the above value is an indication and can be used with confidence under the stated conditions.

[2] It is worth noting that the boxed guideline values in Eurocode 8 have not been calibrated for Icelandic environments.

Recorded time series and derived data for general reference

It should be pointed out that time series as well as linear spectra from the South Iceland earthquakes in June 2000 are available online at the website: http://www.isesd.hi.is/. This information is also available on a CDROM disk, entitled *European Strong Motion Database*, Vol 2, with non-linear response spectra added among other relevant data.

5.4 Conceptual design consideration for damage tolerant structures

The experience from past strong earthquakes proves that the initial conceptual design of a building is extremely important for the behaviour of the building during an earthquake. The guiding principles governing the initial conceptual design are as follows:

- The aspect of seismic hazard should be taken into account in the early stages of the conceptual design of a building,
- Structure should be simple,
- Structure should be compact and regular in both plan and elevation. Avoid structures with elongated or irregular plans; having substantial setbacks in elevation; or that are unusually slender.
- Avoid unnecessary mass and achieve a uniform distribution of mass.
- Transmission of the seismic (inertia) forces to the ground should be direct and clear, i.e. complete load path.
- Uniformity, symmetry and redundancy should be ensured,
- Structures should be statically undetermined i.e. redundant. Use a backup structural system where ever possible.
- Bi-directional resistance and stiffness should be ensured,
- Torsion resistance and stiffness should be ensured and symmetry preserved (main structural elements should be placed symmetrically nearby periphery of the building),
- Structural elements should be appropriately connected with floor systems or diaphragms (which have to have sufficient in-plane stiffness),
- Building should have adequate foundation.
- Use a uniform and continuous distribution of stiffness and strength. Avoid non-structural components that unintentionally effect this distribution. Avoid sudden changes in member sizes or details.

- Permit inelastic action (damage) only in inherently non-critical ductile elements (i.e., in beams rather than columns).
- Detail the members to avoid premature, brittle failure modes. Utilize capacity design principles to avoid undesired shear, axial or joint failures and to foster ductile flexural failure modes in the event of accidental overloads.
- Avoid hammering (pounding) of adjacent structures.
- Tie all structural components together. Anchor non-structural components to structure to avoid falling hazards**.**
- Avoid systems with low amounts of viscous damping. Absence of non-structural components tied to structure may be indication of low damping in steel structures.

In this context it is worth mentioning that softening of the structural system may often be more beneficial than strengthening (Bachmann, 2002).

6. DISCUSSION AND REMARKS

Results of a preliminary probabilistic seismic hazard analysis for an industrial lot at Bakki, near Húsavík, in North Iceland, are presented. The analysis is applied to derive peak ground acceleration values and acceleration response ordinates corresponding to 10% probability of exceedance in 50 years. The inelastic response has also been studied and acceleration response ordinates for stiff and flexible system, respectively, presented.

It should be noted that the duration of strong shaking is relatively short for the study site. The dynamic amplification of earthquake induced response tends to be higher for events with the long duration, than for those with shorter durations. It is also worth noting the rapid attenuation of spectral acceleration ordinates with increasing source distance. These aspects have an effect on both the spectral acceleration ordinates and the structural behaviour factors. It is worth underlining that the result is a significant reduction in computational earthquake design action compared to using the uncalibrated box table values provided in Eurocode 8.

In the present study only point sources have been included. Furthermore, only point sites have been studied without taking into consideration the finite dimensions of the proposed buildings and the spatial variation in ground motion.

Comments on spatial variation of wave motion

The current engineering practice assumes most commonly that:

- excitations at all support points are the same; or
- excitations at different support points are only delayed by a phase difference induced by the wave propagation

In other words the earthquake action at all support points is assumed to be fully *coherent*. This is a great simplification as earthquake accelerograms measured at different locations within the dimensions of an engineered structure are typically different. In view of that it is reasonable to ask whether or not the differences in earthquake accelerograms over the dimensions of engineered structures can be neglected? In current engineering practice it is usually regarded as reasonably conservative to neglect these effects? However, to answer this question rationally a careful analysis has to be carried out in each case to meet the Eurocode 8 requirements of taking these effects into consideration.

The spatial variability of earthquake ground motion is due to different effects the most important of which are the following:

- *Wave passage effect:* Seismic waves arrive at different times at different foundation points.
- *Incoherence effect:* Differences in the manner of superposition of waves (a) arriving from an extended finite source, and (b) scattered by irregularities and inhomogeneities along the path and at the site, which causes a loss of coherency.

- *Local site effect:* Differences in local soil conditions under the foundation may alter the amplitude and frequency content of the bedrock motions differently.

The incoherence effect will in general tend to reduce the earthquake action in the superstructure while the wave passage effects may increase the forces acting on the foundation walls. The incoherence effects are greatest for stiff structure while the greatest wave passage effects are usually thought induced by long periodic wave components. At this point it is not possible to conclude that these effects can be neglected without carrying out a detailed study of the actual structure.

De-aggrigation

The discussion so far has concentrated chiefly on uniform hazard spectrum for the study site, accounting for all probable events. However, a real structure constructed at the study site will never experience such action as described by the uniform hazard spectrum. The structure will only be subjected to one major earthquake at the time and most probably only one major earthquake during its entire functional live. Therefore it is of interest to know which type of earthquake that might be, i.e. what magnitude would it have and what would be the distance to the source. Obviously these questions are related to the basic seismo-tectonic model at hand and the hazard or the probability level adopted. The solution to this problem is furnished in what has been called de-aggregation of seismic hazard. By de-aggregation it is possible, by following the computations when constructing the hazard curve, to determine what event is contributing most to specified spectral ordinates corresponding to a given probability level.

Based on limited de-aggregation analysis for 500 year return period a moderate sized earthquake at a small distance from the site is expected to contribute most to the peak ground acceleration as well as the spectral acceleration of lightly damped stiff linear elastic system. However, a bigger earthquake located at a greater distance from the site is expected to contribute most to the horizontal spectral acceleration of lightly damped flexible linear elastic system.

At the 500 year probability level the earthquakes likely to have effects at the Bakki site originate on the Flatey lineation and the Grímsey lineation, while the Dalvík lineation and the spreading zone contributes little. However, at other probability levels this may be different.

The effect of the Flatey seismic lineation

The seismic activities at the so-called Flatey delineation dominate the earthquake action on stiff (low-rise) structures at the study site. In this context, it is, however, worth pointing out that the assumed seismic activity has been assumed uniform over the whole length of the delineation, which is apparently contradicted by observations (see Sæmundsson, 2007). It is found that the seismic activity on the segment from south of the Flatey Island and through the Húsavík Area has been less active than the northern part of the delineation. If this observation is accounted for in the hazard calculations it is

found that the spectral acceleration ordinates for stiff structures are reduced by a factor two. That is, the suggested design action of 35% g (corresponding to ductility ratio equal to 2) would become about 18% g. Therefore, it would be beneficial if it were possible to define more precisely the seismic activity on the delineation closest to the proposed industrial lot.

Suggested future tasks

So far the presented work has been concentrating on the development of preliminary simplified probabilistic estimates on horizontal and vertical earthquake action. In the development many assumptions have been made, which most likely lead to a conservative estimates of the suggested design values. Therefore, it is judged necessary to refine the study using more advanced methods and models, such as point-source models and finite-source models along with additional earthquake data from available databanks for further verification of the applied regression model. Fault rupture effects on surface motion should also be included.

The main themes are assumed to be as follows:

- Detailed analysis of potential earthquake sources including re-assessment of historical events
- Re-assessment of hazard curves for linear elastic response spectrum
- Hazard curves for non-linear response spectrum ordinates for selected range of undamped natural periods and 5% critical damping ratio. Both constant strength and constant ductility spectrum will be considered
- De-aggrigation of seismic hazard
- Duration of earthquake motion
- Spatial structure of earthquake motion
- Differential motion emphasising velocity and displacement
- Behaviour of second order systems including nonlinear effects
- Simulated time series to be used in design considerations and analysis. Special emphasis will be put on attenuation and directionality representing near-field, intermediate and far field effects.
- Final earthquake design specifications accounting for performance requirements specified by the owner.

A prerequisite required to make this additional study as objective as possible are information on details of the proposed structures to be erected on the industrial lot.

REFERENCES

Aki, K. 1994. Analyzing Probabilistic Seismic Hazard Analysis. *Civil Engineering* 64(2), 28-29.

Aki, K. and Richards, P., 1980. *Quantitative Seismology, Theory and Methods*. Freeman and Company, San Francisco.

Ambraseys, N. N. et al., 2005, Equations for the Estimation of Strong Ground Motions from Shallow Crustal Earthquakes Using Data from Europe and the Middle East: Horizontal Peak Ground Acceleration and Spectral Acceleration. *Bulletin of Earthquake Engineering*, **3** (1). Pages 1-53.

Ambraseys, N. N. et al., 2005, Equations for the Estimation of Strong Ground Motions from Shallow Crustal Earthquakes Using Data from Europe and the Middle East: Vertical Peak Ground Acceleration and Spectral Acceleration. *Bulletin of Earthquake Engineering*, **3** (1), Pages 55-73.

Ambraseys, N. N., Douglas, J., Sigbjörnsson, R., Berge-Thierry, C., Suhadolc, P., Costa, G., Smit, P. M., 2004. *European strong-motion database using strong-motion datascape navigator: Users manual*. London: Imperial College of Science, Technology and Medicine.

Ambraseys, N. N., Douglas, J., Sigbjörnsson, R., Berge-Thierry, C., Suhadolc, P., Costa, G., et al., 2004. Dissemination of european strong-motion data, volume 2. In *Proceedings of the13th World Conference on Earthquake Engineering* (pp. 13). Vancouver: Mira.

Ambraseys, N. N., Sigbjörnsson, R., 2000. *Re-appraisal of the seismicity of Iceland*, Earthquake Engineering Research Centre, Selfoss, June 2000, ISBN 9797-989-91-4X, 196 pages.

Ambraseys, N. N., Sigbjörnsson, R., 2003. On *the seismicity of northwestern Europe*, Imperial College London, Department of Civil & Environmental Engineering, Soil Mechanics, Research report number: 03-001-SM, 116 pages.

Ambraseys, N. N., Smit, P. M., Douglas, J., Margaris, B., Sigbjörnsson, R., Ólafsson, S., et al., 2004. Internet site for European strong-motion data. *Bollettino di Geofisica Teorica ed Applicata*, **45**(3), 113-129.

Ambraseys, N. N., Smit, P., Sigbjörnsson, R., Suhadolc, P., and Margaris, B. 2002. *Internet-Site for European Strong-Motion Data*. (http://www.ISESD.hi.is), European Commission, Research-Directorate General, Environment and Climate Programme

Ambraseys, N., Douglas, J., Sigbjörnsson, R., Berge-Thierry, C., Suhadolc, P., Costa, G., et al., 2004. *European Strong-Motion Database* (Vol. 2). London: Imperial College.

Anderson, J. G. & Hough, S. E. (1984), A model for the shape of the Fourier amplitude spectrum of acceleration at high frequencies, *Bull. Seism. Soc. Am.* 74, 1969-1993.

Barroso, L. R. & Winterstein, S. 2002. Probabilistic seismic demand analysis of controlled steel moment-resisting frame structures. *Earthquake Engineering & Structural Dynamics* **31**(12), 2049-2066.

Bazzurro, P. & Cornell, C. A. 1994. Seismic Hazard Analysis of Nonlinear Structures .2. Applications. *Journal of Structural Engineering-Asce* **120**(11), 3345-3365.

Bazzurro, P. & Cornell, C. A. 1999. Disaggregation of seismic hazard. *Bulletin of the Seismological Society of America* **89**(2), 501-520.

Bender, B., 1984. Incorporating Acceleration Variability into Seismic Hazard Analysis, *Bulletin of the Seismological Society of America*, **74**, 1451-1462.

Björnsson, A. (1985). Dynamics of crustal rifting in NE Iceland. *Journal ofGeophysical Research*. 90 (B12), p. 10151–10162.

Boore, D. M. 1983. Stochastic simulation of high-frequency ground motions based on seismological models of the radiated spectra. *Bulletin of the Seismological Society of America*, **73**(6), 1865–1894.

Boore, D. M., & Joyner, W. B. 1982. The empirical prediction of ground motion. *Bulletin of the Seismological Society of America*, **72**(6), S43–S60. Part B.

Brandsdóttir, B., Einarsson, P., Detrick, R., Mayer, L., and Calder, B. (2003). Lost in Iceland: Fracture zone complications along the Mid-Atlantic Ridge plate boundary. *Eos Trans. AGU 84, (46)*, Abstract F1370.

Brandsdóttir, B., Gudmundsson, G., Kjartansson, E., Helgadóttir, G., Richter, B., Detrick, R., Slunga, R., Riedel, C. (2005). Hafsbotninn og jarðskjálftar í Tjörnesbrotabeltinu. *Vorráðstefna 2005. Ágrip erinda og veggspjalda. Jarðfræðafélag Íslands,* 22 p.

Brandsdóttir, B., Richter, B., Riedel, C., Dahm, T., Helgadóttir, G., Kjartansson, E., Detrick, R., Magnússon, A., Asgrímsson, A., Palsson, B., Karson, J.,Saemundsson, K., Mayer, L., Calder, B., and Driscoll, N. (2004). Tectonic Details of the Tjörnes Fracture Zone, an Onshore-Offshore Ridge-Transform in N-Iceland. *Eos Transactions of the American Geophysical Union, 85* (47), Fall Mtg., Suppl., Abstract T41A-1172.

Brune, J. N. (1970), Tectonic stress and the spectra of seismic shear waves from earthquakes, *J. Geophys. Res.* **75**, 4997-5009.

Brune, J. N. 1970. Tectonic stress and the spectra of seismic shear waves from earthquakes. *Journal of Geophysical Research*, **75**(26), 4997–5009.

Brune, J. N. 1971. Correction. *Journal of Geophysical Research*, **76**(20), 5002.

Brune, J. N. 1976. The physics of earthquake strong motion. *Chap. 4, pages 71–139 of:* Lomnitz, C., & Rosenblueth, E. (eds), *Seismic Risk and Engineering Decisions*. Elsevier Scientific Publishing Company.

Campbell, K. W., 1985. Strong Motion Attenuation Relations: A Ten-Year Perspective, *Earthquake Spectra,* **1**, 759-804.

Chapman, M. C., 1995. A Probabilistic Approach to Ground-Motion Selection for Engineering Design, *Bulletin of the Seismological Society of America,* **85**, 937-942.

Convertito, V. & Herrero, A. 2004. Influence of focal mechanism in probabilistic seismic hazard analysis. *Bulletin of the Seismological Society of America* **94**(6), 2124-2136.

Coppersmith, K. J., 1991. Seismic Source Characterization for Engineering Seismic Hazard Analysis, in *Proceedings of the Fourth International Conference on Seismic Zonation,* Vol. 1, 1991, Stanford, CA, Earthquake Engineering Research Institute, Oakland, CA, pp. 3-60.

Cornell, C. A. and Vanmarcke, E. H., 1969. The Major Influences on Seismic Risk, in *Proceedings of the Fourth World Conference of Earthquake Engineering,* Vol. 1, Santiago, Chile, pp. 69-83.

Cornell, C. A. and Winterstein, S. R., 1988. Temporal and Magnitude Dependence in Earthquake Recurrence Models, *Bulletin of the Seismological Society of America*, **78**, 1522-1537.

Detrick, R., Brandsdóttir, B., Driscoll, N., Richter, B., Mayer, L., Fornari, D., Calder, B., and Kent, G. (2003). The tectonic evolution of the Tjörnes Fracture Zone, offshore northern Iceland – ridge jumps and rift propagation. *Eos Trans. AGU 84,* (46), Abstract F1364.

Douglas, J. 2003. Earthquake ground motion estimation using strong-motion records: A review of equations for the estimation of peak ground acceleration and response spectral ordinates. *Earth-Science Reviews*, **61**(1–2), 43–104.

Douglas, J., 2004. Ground motion estimation equations 1964–2003. Reissue of ESEE Report No. 01-1: 'A comprehensive worldwide summary of strong-motion attenuation relationships for peak ground acceleration and spectral ordinates (1969 to 2000)' with corrections and additions. Imperial College London, Department of Civil & Environmental Engineering, Soil Mechanics, Research report number: 04-001-SM

Einarsson, P. (1976) Relative location of earthquakes in the Tjörnes Fracture Zone.*Soc. Sci. Islandica, articles V ,* p. 45–60.

Einarsson, P. (1991). Earthquakes and present-day tectonism in Iceland. *Tectonophysics*, 189, p. 261–279.

Fenwick, R., Detrick, R., Driscoll, N., Brandsdóttir, B., Kent, G., and Babcock, J. (2006). Strain accommodation across the Húsavík-Flatey Fault, Geology, submitted.

Fjäder, K., Gudmundsson, A., and Forslund, T. (1994). Dikes, minor faults and mineral veins associated with a transform fault in North Iceland. *Journal of Structural Geology, 16*, p. 109-119.

Flóvenz, Ó. G., Gunnarsson. K. (1991). Seismic crustal structure in Iceland and surrounding area. *Tectonophysics* 189, p. 1-17.

Foulger, G.R. Jahn, C.H. Seeber, G., Einarsson, P. Julian, B.R. & Heki, K. (1992). Post-rifting stress relaxation at the divergent plate boundary in Northeast Iceland. *Nature*, 358, p. 488–490.

Garcia, S. Arnaud, N.O. Angelier, J. (2003). Rift jump process in Northern Iceland since 10 Ma from Ar-40/Ar-39 geochronology. *Earth Planet Science Letters*, 214 (3-4) p. 529-544.

Garcia, S., Angelier, J., Bergerat, F., and Homberg, C. (2002). Tectonic anaysis of an oceanic transform fault zone based on fault-slip data and earthquake focal mecanisms: The Húsavík-Flatey fault zone, Iceland. *Tectonophysics, 344*, 157-174.

Garcia, S., Dhont, D. (2005). Structural analysis of the Husavik-Flatey transform fault and its relationships with the rift system in Northern Iceland. *Geodinamica Acta*, 18 (1). p. 31-41

Giardini, D., Ed., 1999. The Global Seismic Hazard Assessment Program (GSHAP) 1992-1999, *Ann. Geofis.*, **42**(6), 957-1230.

Gudmundsson, A. (1993). On the structure and formation of fracture zones. *Terra Nova*, 5, p. 215–224.

Gudmundsson, A. (2006). Infrastructure and evolution of ocean-ridge discontinuities in Iceland. *Journal of Geodynamics* (in press).

Gudmundsson, A., Brynjólfsson, S., Jónsson, M.Þ. (1993). Structural analysis of a transform fault-rift zone juntion in North Iceland. *Tectonophysic,s* 220, p. 205-221.

Halldorsson, B. and A. S. Papageorgiou (2004). Calibration of the specific barrier model to earthquakes of different tectonic regions, *Bull. Seism. Soc. Am.* (in press).

Halldorsson, P. (2005). *Jarðskjálftavirkni á Norðurlandi*. Veðurstofa Íslands, greinargerð; 05021. 39 p.

Hanks, T. C. and Kanamori, H., 1979. A Moment-Magnitude Scale, *Geophys. Res.*, **84**, 2348-2350.

Hasegawa, H. S. 1975. Seismic ground motion and residual deformation near a vertical fault. *Canadian Journal of Earth Sciences*, **12**(4), 523–538.

http://www.ISESD.hi.is, 2005. *Internet-Site for European Strong-Motion Data*. European Commission, Research-Directorate General, Environment and Climate Programme, 2001.

http://www.isesd.hi.is. See Ambraseys, N., N. et al. (2002). ISESD – Internet Site for European Strong-Motion Data. European Commission, Research-Directorate General, Environment and Climate Programme.

Jouanne, F., Villemin, T., Ferber, V. (1999). Seismic risk at the rift-transform junction in north Iceland, *Geophysical Research Letters,* 26 (24), 3689–3692.

Jouanne, F., Villemin. T., Berger, A., Henriot. O. (2005) Rift-transform junction in North Iceland: rigid blocks and narrow accommodation zones revealed by GPS 1997-1999-2002. Geophysical Journal International, 167, p. 1439-1446.

Kameda, H. 1994. Probabilistic Seismic Hazard and Stochastic Ground Motions. *Engineering Structures* **16**(7), 547-557.

McGuire, R. K. and Barnhard, T. P., 1981. Effects of Temporal Variations in Seismicity on Seismic Hazard, *Bulletin of the Seismological Society of America.*, **71**, 321-334.

McGuire, R. K. and Shedlock, K. M., 1981. Statistical Uncertainties in Seismic Hazard Evaluations in the United States, *Bulletin of the Seismological Society of America*, **71**, 1287-1308.

McGuire, R. K., 1993. *The practice of earthquake hazard assessment*, Denver: IASPEI ESC, p. 284.

McGuire, R. K., 1995, PSHA and Design Earthquakes: Closing the Loop, *Bull. Seismol Soc. Am.*, **85**, 1275-1284.

McGuire, R. K., 1995. Probabilistic Seismic Hazard Analysis and Design Earthquakes - Closing the Loop. *Bulletin of the Seismological Society of America* **85**(5), 1275-1284.

McGuire, R. K., 2001. Deterministic vs probabilistic earthquake hazards and risks, *Soil Dynamics and Earthquake Engineering*, **21**, 377-84.

McGuire, R. K., 2004. *Seismic Hazard and Risk Analysis*. Earthquake Engineering Research Institute.MNO-10.

Ólafsson, S. & Sigbjörnsson, R. (2004). Attenuation of strong ground motion in shallow earthquakes, *Proc. of the 13th World Conf. on Earthquake Eng*., Vancouver, Canada, August 1.-6., (Paper No. 1616).

Ólafsson, S. (1999) *Estimation of Earthquake-Induced Response*, doctoral thesis, Norwegian University of Science and Technology (NTNU), Sondheim, Norway, (140 pages).

Ólafsson, S. and Sigbjörnsson, R., 1995. Application of ARMA models to estimate earthquake ground motion and structural response, *Earthquake Engineering and Structural Dynamics*, **24**, pp. 951-966.

Ólafsson, S. and Sigbjörnsson, R., 1999. A theoretical attenuation model for earthquake-induced ground motion, *Journal of Earthquake Engineering*, **3**(3), pp. 287-315.

Ólafsson, S., 1999. *Estimation of Earthquake-Induced Response*. Doctoral thesis, Norwegian University of Science and Technology, Trondheim, Norway, 1999.

Ólafsson, S., and Sigbjörnsson, R., 2004. Attenuation of strong ground motion in shallow earthquakes. In *Proceedings of the 13th World Conference on Earthquake Engineering* (pp. 10). Vancouver: Mira.

Ólafsson, S., and Sigbjörnsson, R., 2004. Generation of synthetic accelerograms and structural response using discrete time models. In *Proceedings of the 13th World Conference on Earthquake Engineering* (pp. 15). Vancouver: Mira.

Ólafsson, S., Remseth, S. and Sigbjörnsson, R., 2001. Stochastic models for simulation of strong ground motion in Iceland, *Earthquake Engineering and Structural Dynamics*, **30**, 27 pages.

Ólafsson, S., Sigbjörnsson, R. and Einarsson, P., 1998. Estimation of source parameters and Q from acceleration recorded in the Vatnafjöll Earthquake in South Iceland, *Bulletin of the Seismological Society of America*, **88**(2), pp. 556-563.

Oliveira, C. S., Sigbjörnsson, R., and Ólafsson, S.,2004. A comparative study on strong ground motion in two volcanic environments: Azores and Iceland. In *Proceedings of the 13th World Conference on Earthquake Engineering* (pp. 13). Vancouver: Mira.

Reiter, L, 1990. *Earthquake Hazard Analysis: Issues and Insights*, Columbia University Press, New York.

Rögnvaldsson, S., Gudmundsson, A., and Slunga, R. (1998). Seismotectonic analysis of the Tjörnes Fracture Zone, an active transform fault in North Iceland. *Journal of Geophysical Research, 103*, p. 30117-30129.

Sæmundsson, K. (1974). Evolution of the axial rift zone in northern Iceland and the Tjörnes Fracture Zone. *Geological Society of America Bulletin*, 85, p. 495-504.

Sæmundsson, K., Karson, A,K. (2006): *Stratigraphy and Tectonics of the Húsavík-Western Tjörnes Area*. ÍSOR-2006/032, 2006.

Sigbjörnsson, R. & Ólafsson, S. (2004). On the South Iceland earthquakes in June2000; Strong-motion effects and damage, *Bollettino di Geofisica Teorica ed Applicata*, **45**, 131-152.

Sigbjörnsson, R., 1990. Strong Motion Measurements in Iceland and Seismics Risk Assessment, *Proceedings of the Ninth European Conference on Earthquake Engineering*, The Kucherenko Tsniisk of the USSR Gosstroy, 10 pages.

Sigbjörnsson, R., and Ólafsson, S., 2004. On the South Iceland earthquakes in June 2000: Strong-motion effects and damage. *Bollettino di Geofisica Teorica ed Applicata*, **45**(3), 131-152.

Sigbjörnsson, R., Baldvinsson, G. I. and Thráinsson, H., 1996. The mapping of seismic hazard using stochastic simulation and geographic information system, *Proceedings of the Eleventh World Conference on Earthquake Engineering*, Pergamon.

Sigbjörnsson, R., et al., 1994. On seismic hazard in Iceland - A stochastic simulation approach, *Proceedings of the 10th European Conference on Earthquake Engineering*, Balkema, Rotterdam / Brookfield, pp. 111-116.

Snæbjörnsson, J. T. and Sigbjörnsson, R. 2005. *Kárahnjúkar hydroelectric project. Hálslón area: Assessment of crustal deformations and fault movements.* (Draft Report)

Snæbjörnsson, J. T., Ólafsson, S. and Sigbjörnsson, R. 2005. *Kárahnjúkar hydroelectric project. Hálslón area: Assessment of earthquake action.* Report prepared for the National Power Company of Iceland.

Snæbjörnsson, J. T., Sigbjörnsson, R., and Ólafsson, S., 2004. Modelling of earthquake response spectra for strike-slip earthquakes in the near- and far-field. In *Proceedings of the 13th World Conference on Earthquake Engineering* (pp. 10). Vancouver: Mira.

Sólnes, J., Sigbjörnsson, R., and Elíasson, J., 2004. Probabilistic seismic hazard mapping of Iceland: Proposed seismic zoning and de-aggregation mapping for EUROCODE 8. In *Proceedings of the 13th World Conference on Earthquake on Earthquake Engineering* (pp. 14). Vancouver: Mira.

Sólnes, J., Sigbjörnsson, R., Elíasson, J., 2002. Mapping of earthquake induced risk in Iceland. In: *Proceedings of the 12th European Conference on Earthquake Engineering*, London, UK. Paper no. 215. Oxford: Elsevier Science.

Tenhaus, P. C. and Campbell, K. W., 2003, Seismic Hazard *Analysis.* In *Earthquake Engineering Handbook*, W-F Chen and C. Scawthorn (ed.). CRC Press.

Todorovska, M. I., & Lee, V. W. 1995. A note on sensitivity of uniform probability spectra on modeling the fault geometry in areas with a shallow seismogenic zone. *European Earthquake Engineering*, **IX**(5), 14–22.

Tsai, C. C. P. 1998. Engineering ground motion modeling in the near-source regime using the specific barrier model for probabilistic seismic hazard analysis. *Pure and Applied Geophysics* **152**(1), 107-123.

Vanmarcke E. H. and Lai, S. P. 1980. Strong motion duration and rms amplitude of earthquake records, *Bulletin of the Seismological Society of America*, **70**, 1293-1307.

Wells, D. L. and Coppersmith, K. J., 1994. New Empirical Relationships among Magnitude, Rupture Length, Rupture Width, Rupture Area, and Surface Displacement, *Bulletin of the Seismological Society of America.*, **84**, 974-1002.

Woo, G. 1996. Kernel estimation methods for seismic hazard area source modeling. *Bulletin of the Seismological Society of America* **86**(2), 353-362.